Tectonic evolution of the abrupt northern termination of the Sistan Suture zone (eastern Iran)

Emad Rojhani[a, e], Farzin Ghaemi*[a], Sasan Bagheri[b], Shihu Li[c], Nalan Lom[d],[e] , Douwe J.J. van Hinsbergen[e]

[a]Department of Geology, Faculty of Science, Ferdowsi University of Mashhad, (Mashhad), Iran,

[b]Department of Geoscience, Faculty of Science, University of Sistan and Baluchestan, (Zahedan), Iran,

[c]State Key Laboratory of Lithospheric and Environmental Coevolution, Institute of Geology and Geophysics, Chinese Academy of Sciences, Beijing, 100029, China,

[d]Institute of Earth Sciences, Heidelberg University, Heidelberg, 69120, Germany

[e]Department of Earth Sciences, Utrecht University, Utrecht, the Netherlands,

Emad Rojhani: Writing - Original Draft, Formal analysis, Investigation **Farzin Ghaemi**: Supervision, Funding acquisition **Sasan Bagheri**: Conceptualization, Methodology, Project administration **Shihu Li**: Resources, Investigation, Review & Editing, **Nalan Lom**: Methodology, Writing - Review & Editing **Douwe j.j. van Hinsbergen**: Conceptualization, Writing - Review & Editing, Investigation, Project administration.

Corresponding author: Farzin Ghaemi (fghaeemi@um.ac.ir)

Highlights:

- Eastern Iran evolution is mainly affected by the westward extrusion of western Tibet.
- Sistan suture terminates to the north to a subduction transform edge propagator.
- Two main folding phases deformed the Lut block margin since the middle Eocene.
- Radial dikes on the margin of the Lut block caused by an Oroclinal buckling.

Abstract

The Sistan Suture Zone in eastern Iran hosts the remains of an ocean basin that subducted between the Iranian Lut Block and the Afghan (or Helmand) Block in late Cretaceous to early Eocene time. Surprisingly, this suture zone is N-S trending, nearly perpendicular to and north of the overall E-W trending Neo-Tethyan suture zone that represents the main regional subduction system for most of the Mesozoic and Cenozoic. In this paper, we study the tectonic structure and evolution of the abrupt northern termination of the Sistan suture zone, which holds key clues for the kinematic evolution of its subduction history. We show that the main N-S trend of the suture is defined by folds and thrusts of a westward and structurally downward-younging ocean-derived accretionary prism that abruptly ends against the steep Madar-Kuh thrust. This thrust strikes nearly perpendicular to the Sistan accretionary prism. It disappears towards the southwest, where also the accretionary prism disappears, but continues beyond the suture zone towards the northeast. It places continental rocks of the Lut block southwards over the oceanic domain. We show that a thrust-parallel set of folds and thrusts was cut by strike-perpendicular dikes, and that folds and dikes together were refolded, giving the Madar-Kuh Fault a modern curvilinear trend. U/Pb ages of the dikes of 51.28±1.5 Ma and 43.10±0.51 Ma show that refolding occurred after the Sistan Suture closure. During Sistan ocean subduction, the Madar Kuh Fault was a trench-perpendicular, straight fault at which subduction terminated: we interpret this fault as a transform fault that acted as a STEP fault accommodating westward motion of the Helmand Block into the Iranian back-arc region. This motion was likely accompanied by large-scale, regional block rotations, as previously postulated. Our findings provide key clues on microplates and continents that converged and collided and highlight that major and long-lived E-W component of tectonic motion along the southern Eurasian margin occurred away from western Tibet and into the Iranian back-arc basins, impacting the tectonic evolution of the Iranian and Tibetan plateaus alike.

Keywords: Tibetian extrusion, Orocline test, Sistan suture zone, subduction transform edge propagator (STEP),

1. Introduction

Several major orogenic belts that formed during closure of the Neo-Tethys experienced lateral extrusion of upper plate, orogenic lithosphere. Well-known examples are Anatolia migrating westward away from the Arabia-Eurasia collision zone (Jackson & McKenzie, 1984), the eastern Alps and northern Pannonian basin escaping from the Adria-Eurasia collision zone (Ratschbacher et al., 1991, 1989), and Indochina escaping eastwards from the India-Asia collision zone (Tapponnier et al., 1982; Richter and Fuller, 1996; Li et al., 2017). This lateral escape accommodates crustal shortening and is accommodated along major strike-slip systems that, when active, pose major seismic hazard.
A possible fourth major region of past lateral escape lies to the west of India and Tibet and comprises much of Afghanistan and eastern Iran. Tapponnier et al. (1980) already noticed that the first-order structural architecture of strike-slip faults surrounding the Helmand Block that occupies much of Afghanistan bear characteristics of westward escape, but because scarcity of geological data from this region has prohibited the development of quantitative restorations of westward motion of the Helmand block.

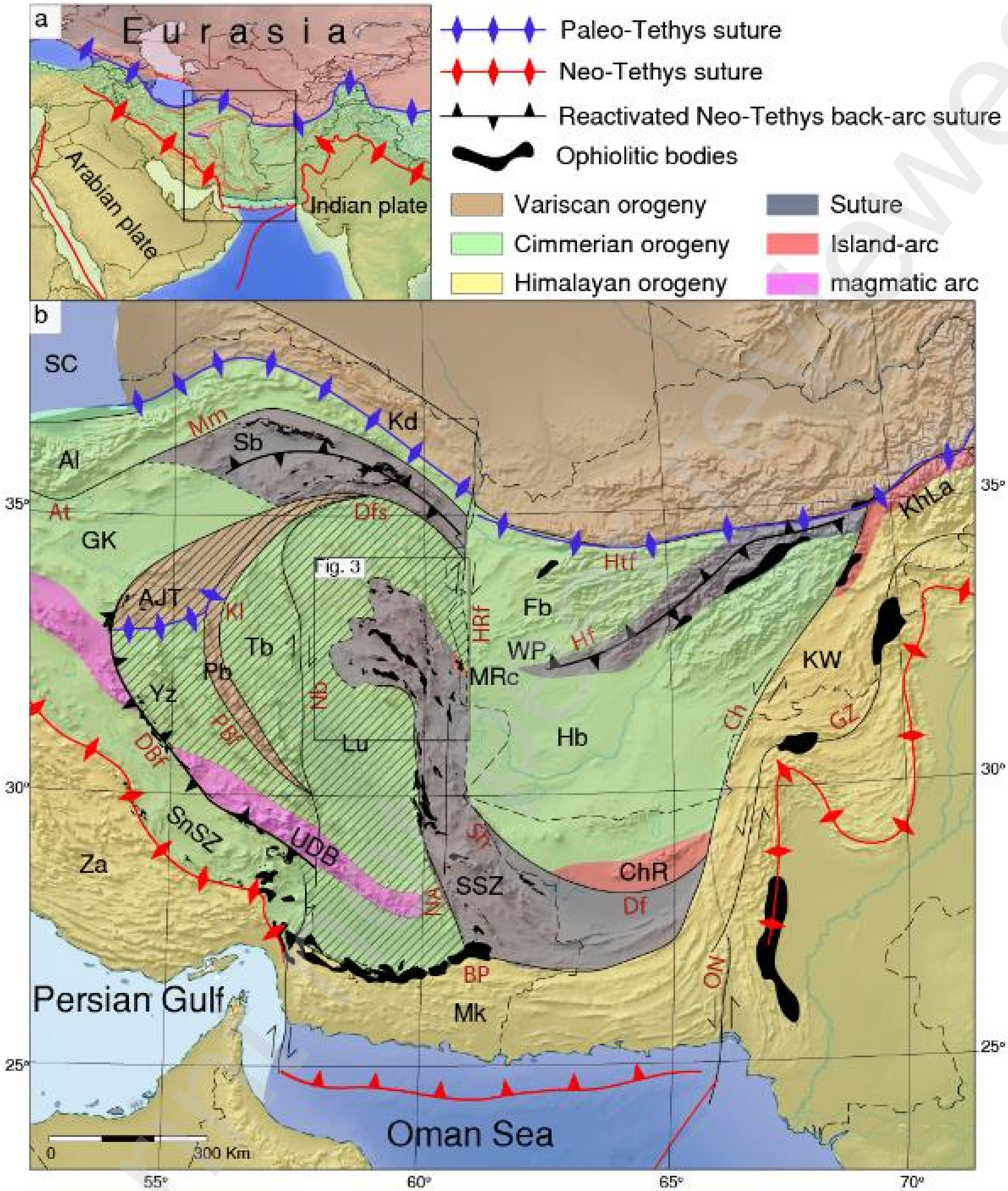

Figure 1. a) Location of the Sistan suture zone in within the Cimmerian terrane and in the Neo-Tethyan territory; b) Sistan Suture zone and surrounding blocks; AJT: Anarak-Jandagh terrane, Al: Alborz, Chagai-Raskoh arc, Fb: Farah basin, GK: Great Kavir, Hb: Helmand block, Kd: Kopeht Dagh, KhLa: Kohistan-Ladakh arc, KW: Katawas flysch basin, Lu: Lut block, Mk: Makran accretionary prism, MRc: Mahi-Rud complex, Pb: Posht-e-Badam, Sb: Sabzevar, Sc: South Caspian sea, SnSz: Sanandaj-Sirjan zone, SSZ: Sistan suture zone, Tb: Tabas block, WP: Waras-Panjaw, Yz: Yazd block; and main faults; At: Atari fault, BP: Bamposht Thrust, DBf: Dehshir-Baft fault, Dfs: Dorouneh fault system, Htf: Herrat fault, HRf: HariRud fault system, Kh: Kahourak fault, Kl: Kalmard fault, Mm: Mayami fault, Nb: Naybandan fault, NA, Nosratabad fault, Nh: Neh fault, PBf: Poshte-Badam fault, Sh: Siahan fault.

The geology of eastern Iran, however, may shed light on the role of lateral escape of the Helmand Block. The Sistan Suture of eastern Iran is a prominent but enigmatic, 800 km long, N-S trending suture zone that forms the modern western boundary of the Helmand Block and separates it from the Lut block of Central Iran (Figure 1). Such a N-S trending suture zone is surprising because closure of the Neo-Tethys ocean has been dominated by N-S convergence and E-W trending subduction zones throughout much of the Mesozoic and Cenozoic. Structural geological observations and distributions of metamorphic and arc magmatic rocks have led previous workers to propose either west or east-dipping subduction as driver to close the Sistan suture zone, or both (Agard et al., 2009; Angiboust et al., 2013; Arjmandzadeh et al., 2011; Bröcker et al., 2013; Pang et al., 2011; Saccani et al., 2010; Tirrul et al., 1983; Bagheri and Damani Gol, 2020). Estimated ages suggest closure between late Cretaceous and late Eocene or Oligocene time (Bröcker et al., 2013; Tirrul et al., 1983; Zarrinkoub et al., 2012), and the onset is often suggested to be Late Cretaceous (Brocker et al., 2013, Jentzer et al., 2022), although others used magmatic and metamorphic records and deformation of the eastern margin of the Lut block to argue for subduction already in Jurassic time (Beydokhti et al., 2015; Esmaeily et al., 2005; Karimpour et al. 2011; Nabiei & Bagheri, 2013; Pang et al., 2013; Stöcklin et al., 1972).
Closure of the Sistan suture by E-W convergence would require major convergence between the Lut block and the Helmand block that was sub-parallel to the overall E-W trending southern Eurasian active margin, this would restore the Helmand block towards the east, i.e., into the Karakoram-Tibetan realm. Such motions have mostly been conceptually inferred without detailed reconstruction, and in absence of further kinematic constraints the magnitude of Helmand extrusion is difficult to constrain. Bagheri and Damani Gol (2020) recently hypothesized that the Sistan suture zone was originally the ~E-W striking Neo-Tethyan trench that became oroclinally buckled over 180° (Figure 2.a). If correct, such a scenario that would allow quantifying extrusion timing and amount and establish kinematic and dynamic relationships between the tectonic and geodynamic evolution of Iran and the western Tibetan plateau.

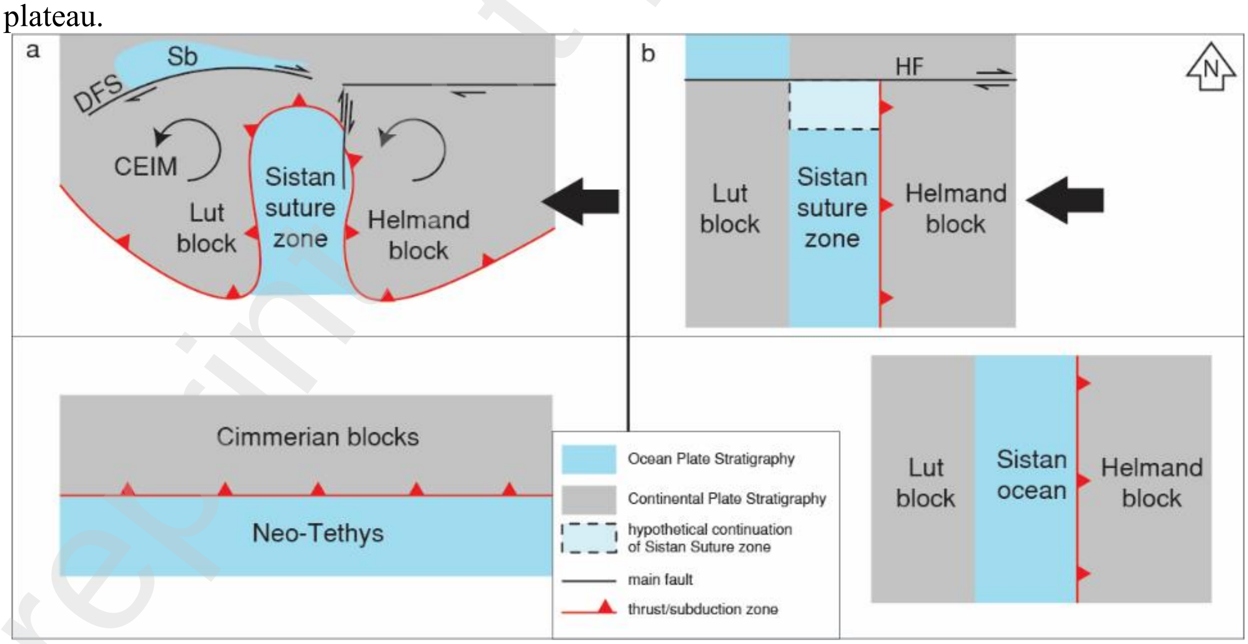

Figure 2. Simplified cartoon of two alternative explanations for northern termination of Sistan suture zone, a) oroclinal buckling, b) westward migration by transform faults. CEIM: Central-east Iranian Microcontinent, Sb: Sabzevar basin; main faults: DFS: Dorouneh Fault System, HF: Herat Fault.

The oroclinal bending hypothesis comes with specific predictions for the tectonic architecture for the northern termination of the Sistan suture zone. It suggests a tightly curved belt that links the eastern margin of the Lut block to the western margin of the Helmand block. This hypothesis allows explaining the Triassic-Paleogene CCW rotation of the Lut bock, inferred from paleomagnetic data (Bina et al., 1986; Davoudzadeh et al., 1981; Soffel et al. 1996). If the alternatively, of the Sistan suture is not the result of oroclinal buckling but was always N-S striking, it either continued farther north than generally mapped (Rossetti et al., 2010), or ends against a transform plate boundary in the north that bounds an extruding domain that includes the Helmand Block and Farah basin (Figure 2.b). Both scenarios include a major westward motion of Helmand but allow for different timing and amount: if Sistan would always have been a N-S striking subduction zone accommodating closure of an enigmatic back-arc basin, the age of HP/LT metamorphism (~90 Ma, Bröcker et al., 2013b) indicates Helmand extrusion was already underway in the late Cretaceous, well before the inception of India-Asia collision. The oroclinal bending scenario does not exclude a relationship with collision, such as also inferred for Indochina (e.g., Li et al., 2017).

In this paper we perform a field-based study into the structure and evolution of the northern termination of the Sistan suture zone, aiming to establish the location of the former subduction zone, the presence or absence of curvilinear belts surrounding this termination and of strike-slip faults, and on the stratigraphic and magmatic architecture to constrain timing of deformation. We review stratigraphic and structural architecture and add new field observations to evaluate whether the northern termination may be a tight orocline.

2. Geological setting

2.1. “Cimmerian Blocks” and intervening sutures

Most of the territories of Iran and Afghanistan are occupied by continental crustal fragments often referred to as ‘Cimmerian blocks’, which are separated from Eurasian and Arabian continents, and from each other, by suture zones (Krumsiek, 1976; Şengör, 1979, 1984; G. M. Stampfli et al., 1991). These continental blocks mostly have a Precambrian basement (M. Berberian, 1973; Stocklin, 1968, 1974; Stöcklin & Mabavi, 1973) that correlates well with the basement of Gondwanan continents to the south (particularly Arabia) (Gass, 1977), and is markedly different from that of the Eurasia to the north (Bagheri & Stampfli, 2008; Şengör, 1984; Stampfli et al., 1991; Stampfli, 2000; Stocklin, 1974). The suture zone of the Cimmerian blocks with Eurasia in the north contains Paleozoic oceanic rock sequences and is interpreted as the suture where the Paleo-Tethys Ocean was consumed (Şengör, 1979). A suture between the Cimmerian Blocks with the Zagros fold-thrust belt in the south exposes Mesozoic-Cenozoic oceanic rocks, thought to have derived from northward subducted lithosphere of the Neo-Tethys Ocean (Şengör, 1979). The thin-skinned Zagros fold-thrust belt consists of a sequence of Paleozoic-Cenozoic sedimentary rocks that are interpreted to represent the off-scraped, accreted sedimentary cover of the Arabian passive margin (Agard et al., 2009; Allen, 2021; Berberian & King, 1981). Accretion of the Zagros fold-thrust belt occurred during the Neogene following initial collision between Arabian plate and Eurasia after full consumption of the Neo-Tethyan oceanic lithosphere, which probably occurred during the mid-late Oligocene (McQuarrie & Van Hinsbergen, 2013; Pirouz et al., 2017). To the north of the Neo-Tethyan suture lies a belt of Jurassic-Cretaceous metamorphosed and igneous rocks intruded in continental ‘Cimmerian’ basement (the Sanandaj-Sirjan Zone) and adjacent to the north lies the NW-trending Urumieh-Dokhtar magmatic belt, consisting of the Cenozoic calc-alkaline magmatic rocks: these belts are interpreted as the subduction-related magmatic arc that shifted northward in the early Cenozoic (Agard et al., 2011; Allen, 2021; Berberian & Berberian, 1981; Berberian & King, 1981; Ghodsi et al., 2016; Moghadam & Stern, 2015; Şengör, 1990; Stocklin, 1968).

The Cimmerian blocks are thought to have been one contiguous continent that broke off Gondwana-Land in the Permian and drifted north towards Eurasia where it arrived in the Triassic, closing the Paleo-Tethys and opening the Neo-Tethys in its wake (Şengör, 1979; Wan et al., 2021; Şengör et al. 2023). However, the Cimmerian fragments are presently separated by oceanic sutures that contain post-Triassic to Paleogene oceanic rocks interpreted to reflect Mesozoic break-up and reorganization of the once-contiguous Cimmerian block. The Central-East Iranian Microcontinent (CEIM) (Soffel & Förster, 1984) occupies the heart of Iran and is surrounded by a peculiar, oval-shaped belt of ophiolitic mélanges (Figure 1). These ophiolitic belts are accompanied by major fault systems: the Nain-Baft ophiolitic mélange and Dehshir-Baft fault system in south-southwest separate the CEIM from the Sanandaj-Sirjan zone (e.g., Moghadam et al., 2014; Pirnia et al., 2020); the Sabzevar ophiolites and mélanges and the Great Kavir-Dorouneh fault system separate the CEIM from the Alborz mountains in the northwest (e.g., Rossetti et al., 2014; Moghadam et al., 2019), and the Birjand-Nehbandan ophiolites and the NosratAbad Fault system in the east together form the Sistan suture zone that separates the CEIM from the Helmand block and the Lower Mesozoic Farah basin to its north (Stocklin, 1968). The ophiolites are Cretaceous in age and are commonly interpreted to be derived from Cretaceous back-arc basins that formed in the Upper plate of the subducting Neo-Tethyan subduction zone (Baroz et al, 1984; Arvin and Robinson, 1994; Shojaat et al., 2003; Ghazi et al., 2004; Rossetti et al., 2010; Zarrinkoub et al., 2012), although others have argued for scenarios in which some of these ophiolite belts represent the Neo-Tethyan suture (Bagheri & Damani Gol, 2020; Moghadam & Stern, 2015), and some belong to the Paleo-Tethyan suture zone and are displaced to the modern situation (Bagheri & Stampfli, 2008).

The CEIM consists of fault-bounded blocks that expose a Late Precambrian (Pan-African/Cadomian) crystalline basement and a Mesozoic-Cenozoic sedimentary cover. Major strike-slip faults define the Yazd, Tabas, and Lut blocks (M. Berberian & King, 1981; Stocklin, 1968), and the Anarak-Jandagh terrane and the Posht-e Badam block (Bagheri & Stampfli, 2008) (Figure 1). Most of these strike-slip fault systems result from late Neogene deformation (Walker & Jackson, 2004), with the exception of the Anarak-Jandagh terrane and Posht-e Badam block that are separated from the Yazd Block in south by a suture zone with Paleozoic oceanic rocks (S Bagheri, 2007). The former two have a Carboniferous ('Variscan') crystalline basement that contrasts with that of the other continental segments of the other blocks in the CEIM and are interpreted as Eurasian basement, and the suture zone is interpreted as the far-displaced Paleo-Tethys suture. Its presence within the CEIM is interpreted as the result of large-scale Mesozoic-Cenozoic deformation affecting central Iran (Bagheri & Stampfli, 2008; Buchs et al., 2013; Davoudzadeh & Schmidt, 1981; Zanchi et al., 2009, 2015). This is likely associated with a 90° CCW rotation of the CEIM during the Mesozoic (Davoudzadeh et al., 1981; Bina et al., 1986; Conrad et al., 1981; Soffel et al., 1992, 1996), but kinematic restorations of Central Iranian deformation so far remain schematic.

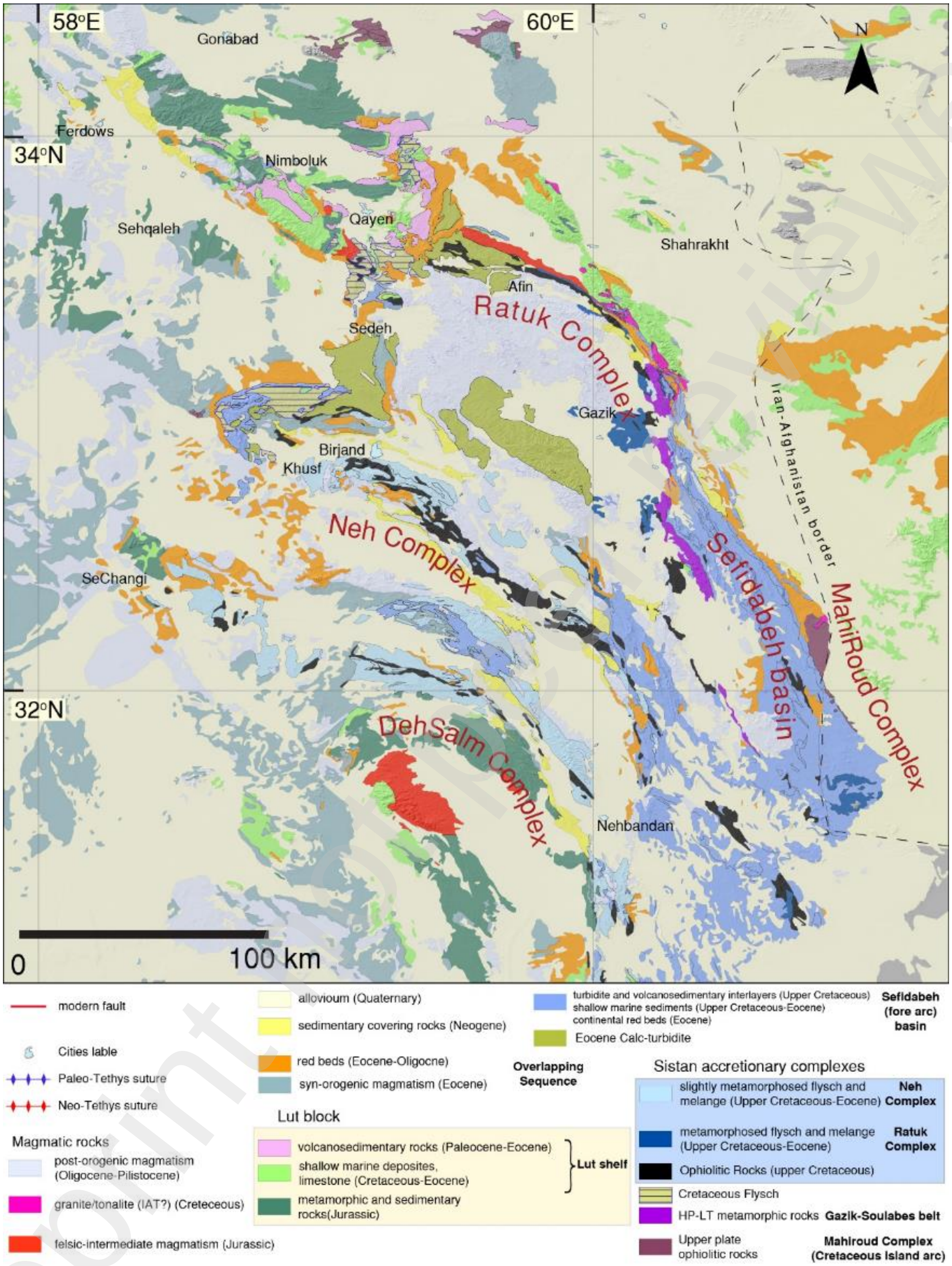

Figure 3. geological map of northern termination of Sistan suture zone, representing geological units of Lut block, Sistan suture and Helmand block, after (Eftekhar-Nezhad and Ruttner, 1977; Alavi-Naini, 1980; Alavi-Naini and Behruzi, 1983; Guillou et al., 1983; Berthiaux et al., 1991; Eftekhar-Nezhad and Stocklin, 1992).

To the east of the Sistan suture lies the Helmand Block of Afghanistan (Figure 1). This also consists of a Precambrian crystalline basement, and is overlain by a Permian-Middle Cenozoic, discontinuous, shallow-water carbonates sequence (Schreiber et al., 1972; Jovan Stöcklin, 1989). The basement of the Helmand Block is, as far as known, similar to the Cimmerian basement of Iran, but also to the basement of the Qiangtang or Lhasa terranes of Tibet. This block is separated from the Eurasian crystalline crust by a wide, Triassic flysch belt associated with ophiolites (e.g. Waras-Panjaw ophiolite) known as the Farah, or Farah Rud basin (Boulin, 1990; Montenat, 2009; Siehl, 2017), which may be equivalent to the Songpan-Garzi flysch belt of Tibet (Girardeau et al., 1989). The Helmand block is separated from the Cretaceous-Paleogene shallow marine sediments of Makran Range in the south (Ahmed 1969; Auden 1974; Falcon 1974, Figure 1), by the Chagai-Raskoh belt that constitutes an accreted intra-oceanic arc (Camp & Griffis, 1982; Jones, 1961; Pudsey, 1986), which may have been contiguous with the Iranian magmatic arc to the west (the Mahi Rud complex), or with the Kohistan-Ladakh arc to the east, now displaced far northwards along the Hari-Rud and Chaman fault respectively (Nicholson et al., 2010; Siddiqui et al., 2017) (Figure 1).

2.2. Architecture of the Sistan Suture zone

The Sistan Suture zone in eastern Iran is a sigmoidal, N-S trending zone with ocean-derived, partly metamorphosed rocks separating the continental Helmand Block in the east from the Lut Block in the west. The suture zone is generally interpreted to have been the locus of subduction that accommodated E-W convergence between the adjacent continental blocks. In the south, the blocks and suture are sealed by the Eocene and younger, E-W trending Makran accretionary prism at the north-dipping Bamposht thrust fault that formed at the modern north-ward dipping subduction zone accommodating Arabian plate subduction (e.g., McCall, 2002; Ninkabou et al., 2021) (Figure 1).

The eastern margin of the suture zone with the Helmand Block is covered by Quaternary alluvium and can nowhere be directly observed. Nonetheless, the prominent, but inactive, Hari Rud-Siahan Fault system is considered as the eastern boundary (Sargazi et al., 2022; Stöcklin, 1989, p. 242). To the west of this Neogene strike-slip fault are exposures of ophiolites and underlying accreted and in part metamorphosed ocean plate stratigraphy, and no continental basement is known.

The tectonostratigraphy of the Sistan Suture zone consists of non-metamorphosed ophiolites with supra-subduction zone geochemical signature to which an arc magmatic complex (the Mahi Rud complex) is accreted, and that is overlain by an Upper Cretaceous to Paleogene marine turbiditic series that includes olistoliths, known as the Sefidabeh forearc basin. Below the ophiolites lie accreted OPS (Oceanic-Plate Stratigraphy) series, in places incorporated in a serpentinite mélange and metamorphosed at high pressure and low temperature (the Ratuk complex). To the west low-grade metamorphosed OPS and ophiolite mélange lie under the Ratuk complex (Neh Complex) (Figure 3).

Oceanic crustal rocks in the Sistan suture are commonly all described as ‘ophiolite’, but comprise both upper-plate derived, SSZ-type ophiolites and downgoing plate-derived accreted OPS sequences with MORB basement (Delavari, 2013). It is not clear from each outcrop of oceanic mafic rocks to which of the two classes they belong, since structural relationships are often challenging to assess due to the Upper Eocene and younger sedimentary cover, as well, the movements of the succedent active strike-slip faults (e.g. the Neh fault system, NosratAbad fault system) (Figure 4). Nonetheless, the presence of SSZ-type ophiolites has been identified through geochemical analysis of the Nehbandan Ophiolite mélange that contains a mantle and crustal section with E-MORB geochemical signature (Karimzadeh et al., 2020; Saccani et al., 2010).

Also, the Siahjangal, Nosrat-Abad, Ophiolites and the Tchehel-Kureh ophiolite (92 ± 3 Ma, K-Ar method) (Delaloye & Desmons, 1980) respectively in the south and central west of the Sistan Suture have geochemical characteristics of SSZ (Delaloye & Desmons, 1980; Moslempour et al., 2012; Nikbakht et al., 2021). The SSZ-type ophiolites are not directly dated, but the oldest overlying sediments that have been found are Turonian pelagic limestones (Tirrul et al., 1983, p. 139) and the SSZ spreading phase is thus thought to be of Late Cretaceous age (e.g., Saccani et al, 2010). Recently, the NE-dipping intra-oceanic subduction zone is interpreted to cause a south-westward obduction and preservation of the ophiolite onto the Lut block (Jentzer et al., 2022). In places, the SSZ ophiolites are intruded by magmatic rocks that may be related to a subduction-related arc. The Nehbandan ophiolite is intruded by the Bibi-Maryam granitoid with a geochemical signature of slab melting in an oceanic arc and a pre-plate collision setting, that yielded a U-Pb zircon age of 58.6 Ma (Delavari et al., 2014). In the easternmost part of the Sistan Suture zone, as well, tonalite stocks of the Mahi Rud complex intrude pillow lavas and interbedded pelagic sediments. These stocks and the mafic host-rocks were originally interpreted as a rift-related magmatic series (the Cheshmeh Ostad Group) (Guillou et al., 1983; Tirrul et al., 1983), but later geochemical work revealed calc-alkaline to tholeiitic magmatic characteristics suggesting that they formed in an arc setting (Keshtgar et al., 2019). The age of the tonalitic granitoids intruded into the ophiolitic rocks revealed by K-Ar dating on amphibole gave 79.4 ± 3.2 to 83.6 ± 2.6 Ma respectively (Maurizot, 1980; Maurizot et al., 1990) and a recent U/Pb zircon age gave 103.9 ± 2.9 Ma (Bagheri & Damani Gol, 2020), giving the oldest known age for the IAT magmatism in the Sistan Suture.

The general westward younging of accreted OPS sequences and overall westward thrust vergence led to the interpretation that the SSZ ophiolites formed adjacent to a NE dipping, intra-oceanic subduction zone that likely formed in the forearc of the Helmand block (Angiboust et al., 2013; Delavari, 2013). The structurally highest, and oldest accreted sequence is the HP-LT of Ratuk complex. The Ratuk complex is exposed in N-S trending massifs bounded by Cenozoic strike-slip faults (Figure 3) (Tirrul et al., 1983) and exposes metamorphosed and dismembered OPS sequences including metabasalt and -spilite, metacherts, and metaflysch at blueschist, eclogite, and amphibolite facies (Bonnet et al., 2018; Fotoohi Rad et al., 2005; Kurzawa et al., 2017). These rocks are mostly exposed as blocks and boulders in a serpentinite mélange thrusted onto a non-metamorphosed mixture of ultramafic and mafic rocks, Cretaceous to Eocene phyllite and Senonian to Maastrichtian pelagic sediments interpreted as OPS sequences of a younger part of the accretionary prism (Agard et al., 2009; Angiboust et al., 2013; Fotoohi Rad et al., 2005). White mica and amphibole Ar/Ar dating of HP metabasites of Ratuk Complex yielded 135 – 125 Ma ages (Fotoohi Rad et al., 2009) but these data were later explained because of argon contamination in high-pressure conditions (Bröcker et al., 2013). Instead, the age of metamorphism was constrained between ~86 and ~75 Ma by, Rb-Sr and Ar-Ar dating of phengite, white mica, garnet, omphacite and albite in the blueschist and eclogite, and by U-Pb dating of zircon grains in the meta-plagiogranite and eclogite (Bröcker et al., 2013; Kurzawa et al., 2017). Age of Cenomanian-Campanian is given from the radiolarian cherts of the Ratuk complex (Babazadeh & De Wever, 2004a, b).

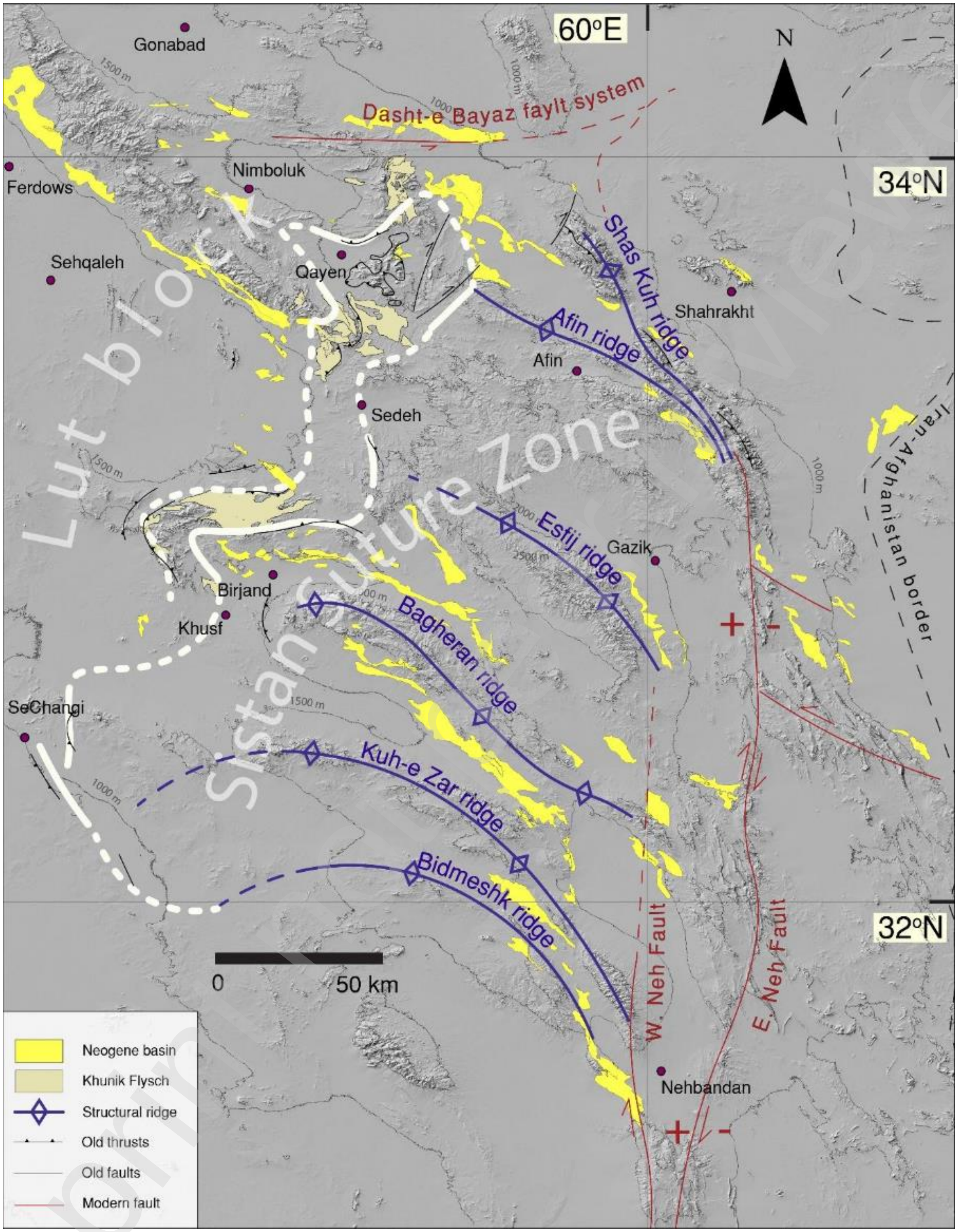

Figure 4. **Digital Elevation Model (DEM) highlighting the northern end of the Sistan suture zone. The yellow polygons mark the narrow Neogene basins trending NW-SE, nestled between structural ridges of the same orientation. The definitive white line represents the distinct boundary against which the Lut block rocks border the structural ridges. Cream-colored polygons showcase the Upper Cretaceous-Paleocene trench-fill flysch (Khunik formation) that runs parallel to this boundary. The thrust faults (thin black lines) that deformed the Sedeh Formation are also parallel to the boundary.**

To the west of the Ratuk complex lies the mostly non-metamorphic Neh complex that contains deformed OPS sequences that include peridotites and mafic rocks of MORB affinity, interpreted as off scraped from subducted oceanic lithosphere. The most prominent mafic-ultramafic units in this accretionary sequence are the Birjand Ophiolite, consisting of serpentinized ultramafic rocks including harzburgite, lherzolite, and pyroxenite associated with gabbros and sheeted diabase, and pelagic clays, with mostly tectonic contacts (Ohanion et al., 1983) (Figure 3). Leuco-gabbro yielded a U-Pb zircon age of ~113 -107 Ma (Zarrinkoub et al., 2012). The ophiolitic mafic rocks of this belt with N-MORB affinity are interpreted to have originated from a depleted mantle (Zarrinkoub et al. 2010). N-MORB geochemical signatures are also found in the south of the Sistan suture as part of the Neh complex (Biabangard et al., 2020; Delaloye & Desmons, 1980; Desmons & Beccaluva, 1983). The ages of radiolarian red clay-rich pelagic sedimentary rocks in south of the Neh complex are Albian-Aptian (Ozsvárt et al., 2020), and Upper Cretaceous-Lower Eocene hemipelagic sediments with slump structures and turbiditic sandstones, weakly metamorphosed (to phyllite and phyllonite), are interpreted as the trench-fill sequence of the OPS (Tirrul et al., 1983). The only records of the Eocene metamorphism are from two area on the west of the Sistan Suture. White mica from the calcschist and sedimentary schist of the Birjand ophiolite and Tchehel-Kureh mélange respectively, yielded ages of 68-65 (K-Ar method) (Delaloye & Desmons, 1980, p. 103). The deformed OPS units are unconformably covered by Upper Eocene shallow-water nummulitic limestone (Eftekhar-Nezhad & Stocklin, 1992; Gholami et al., 2015). This follows by a sequence of Upper Eocene red beds (Rowshanravan et al., 2006) and abundant Oligocene-Pliocene volcanic rocks that are related to plutons of the same age found within the Sistan suture as well as in the neighboring continental units of the Lut block (Pang et al., 2011, 2012). Collectively, these relationships suggest that oceanic spreading of the subducted ocean floor continued until at least ~107 Ma, that eastward (in modern coordinates) subduction in the Sistan subduction zone was underway by 86, and perhaps 103 Ma (corresponding to the oldest age found in the Mahi Rud stocks), and that subduction ceased in the mid-Eocene. After the Middle Eocene, the Sistan Suture was deformed along N-S trending strike-slip faults that include the Hari Rud fault (Figure 1) and the prominent Neh Fault system with dextral displacements of some tens of kilometers (Stocklin, 1968; R. Walker & Jackson, 2004).

The Sefidabeh basin represents more than 8 kilometers of Senonian-Eocene turbiditic sequence and olistostrome reworking ophiolitic rocks and shallow-marine derived limestone, interbedded with calc-alkaline volcanic rocks (Camp & Griffis, 1982; Tirrul et al., 1983). The basement exposure of the oldest unit of the basin is not reported, but the entire succession younger than early Maastrichtian unconformably overlie SSZ-type ophiolitic rocks, island arc rocks intruded into the ophiolites, as well as exhumed sub-ophiolitic mélange with HP-LT metamorphic rocks and the structural highs of the accretionary prisms. The turbidites of the oldest known strata of the Sefidabeh basin, the Lahu Formation, contains pebbles of shallow-water rudist-bearing limestone with and large-foram grainstones yielded an age of Aptian to Cenomanian, but the age obtained from the indigenous planktonic micro fauna is Lower Senonian (Tirrul et al., 1980). To the east the flysch that underlies the Mahi Rud Complex is strongly folded and contains olistoliths of gabbro and serpentinized harzburgite. The minor calc-alkaline intermediate to felsic flows and pyroclastic rocks of the Sefidabeh basin are ascribed as being the effusive products of an arc in the Helmand block, however, several of the basaltic andesite flows with tholeiitic characteristic indicating early stages in development of an incipient island-arc (Camp & Griffis, 1982, p. 237), overlying by shallow-water foraminiferal limestone passing upward to the immature clastic sedimentary rocks of the Upper Paleocene age pinch out and pass into turbidites to the west and can be traced into pelagic sedimentary successions, where they are represented by tuff, volcaniclastic, and limestone turbidites. There are significant amounts of plagioclase and pyroxene-phyric volcanic clasts, diabase, and chert in some beds (Guillou et al., 1983; Tirrul et al., 1980). Paleocene-Lower Eocene reef carbonates cover the calc-alkaline volcano-sedimentary and volcanic rocks.

The Ratuk and Neh complexes are unconformably overlain by clastic red bed deposits of the Baran Formation, the youngest sedimentary rocks of the Sefidabeh basin (Tirrul et al., 1983). These mainly consist of non-marine to lagoonal deposits but in places shallow-marine limestones and dolomites, yielded microfossils indicative of a Middle Eocene age (Maurizot, 1980, p. 96). The basal conglomerate of these red beds consists almost exclusively of pebbles from the underlying Paleocene-Eocene limestones, and clasts of serpentinite (Guillou et al., 1983; Keshtgar et al., 2016). The hiatus at the base of the Baran Formation spans the Upper Ypresian and the Lower Lutetian (Maurizot, 1980; Fauvelet & Eftekhar-Nezhad, 1990).

All the rock units of the Sefidabeh basin older than the Middle Eocene experienced two phases of folding (Freund, 1970; Keshtgar et al., 2016). The Middle Eocene Baran Formation experiences a single folding phase and is unconformably covered by gently dipping volcanic rocks of late Oligocene to early Miocene age (an age of 23.3 ± 6.2 Ma, (K-Ar on hornblende) (Tirrul et al., 1980)). The Oligocene-Neogene continental red-bed sequences are not exposed to the east of the Sistan suture zone in Afghanistan, where they are likely covered by unconsolidated Quaternary alluvium (Kokaly et al., 2013).

2.3. Lut block

The Lut block to the west of the Sistan suture exposes Upper Proterozoic-Cambrian basement overlain by Paleozoic-Cenozoic sedimentary rocks and volcanics (Stöcklin, 1974, 1968; 1981). Triassic-Jurassic marine rocks are partly metamorphosed and locally intruded by Middle Jurassic to Cenozoic intrusions, and overlain by associated volcanic rocks (Esmaeily, 2001; Esmaeily et al., 2005; Moradi Noghondar et al., 2011; Tarkian et al., 1983; Karimpour et al., 2011). These volcanics are interlayered with a thick shallow marine sequence, just west of the Sistan Suture Zone in particular by a thick Upper Cretaceous (Upper Aptian-Cenomanian) Paleocene shelf limestone sequence that are also found to the northeast of the termination of the Sistan suture (Figure 3) (Alavi-Naini, 1980; Alavi-Naini & Behruzi, 1983; Eftekhar-Nezhad & Ruttner, 1977; Kluyver et al., 1983; latifi et al., 2018; Raisossadat et al., 2020). These are overlain by Paleocene carbonates, unconformably overlying Middle Eocene-Oligocene continental red beds and deformed Oligocene-Pliocene volcano-sedimentary rocks (Akrami et al., 2005).

The wider Central Iranian Microcontinent, which consists of several fault-bounded blocks, is bounded from continental Cimmerian units to the north, west, and south by other Cretaceous-Eocene suture zones, Nain-Baft and Sabzevar, whereby the Lut Block was in an upper plate position relative to at least the Nain Baft subduction zone (Figure 1) (Shirdashtzadeh et al., 2022). This shows that throughout the closure history of the Sistan Ocean, not only the Helmand Block but also the Lut Block was mobile relative to Eurasia. Paleomagnetic data revealed that the Lut Block underwent counterclockwise rotation throughout much of the Mesozoic-Cenozoic (Conrad et al. 1981; Mattei et al. 2012, 2015; Soffel and Förster, 1980; Soffel et al. 1995), and treating the Sistan Suture Zone in its current orientation as representative for its entire history is therefore a simplification. Nonetheless, the westward, structurally downward propagation of accretion and metamorphism in the Sistan Accretionary Complex suggests that the Lut Block was in a downgoing plate position relative to the Sistan subduction zone.

2.4. The northern termination of Sistan suture

Much of the pre-Eocene geology of the northern termination of the Sistan Suture Zone is covered by a thick sequence of Oligocene-Miocene (27-11 Ma) calc-alkaline volcanic and volcano-sedimentary rocks and associated intrusions (Figure 5). These magmatic rocks are interpreted to originate from post-collisional processes following the Lut-Helmand block collision (Pang et al., 2013 Bagheri and Damani Gol, 2020).

Exposures in erosional windows below this young volcano-sedimentary cover show that the belts that make up the Sistan Suture Zone, i.e. the Ratuk Complex, Neh Complex, and Sefidabeh basin curve in the north of the suture zone into a NW trend (Figure 3). The northeasternmost exposed parts of the Ratuk Complex, forms a narrow NW directed belt of mélange of Cretaceous ultrabasic rocks and red pelagic sediments and Paleocene-Early Eocene turbidites (Fauvelet & Eftekhar-Nezhad, 1990). The northernmost outcrop of the Ratuk complex is overthrust by what we here call the Afin Belt that we infer to be part of the Helmand Block. This consists of Jurassic intermediate volcanic, volcano-sedimentary and intrusive rocks followed by Upper Cretaceous-Paleocene shallow-marine limestones, deformed by NW-SE trending folds and thrusts (Fauvelet & Eftekhar-Nezhad, 1990) (Figure 3).

The Sistan Suture Zone units as well as the Afin Belt are abruptly cut to the NW by a NE-SW-trending curvilinear fault zone and adjacent fold-thrust belt that trends perpendicular to the trend of the Sistan Suture Zone units. To the northwest of this abrupt termination are Paleozoic rocks and Jurassic magmatic-metamorphic rocks of the 'Qaen (Qayen) Allochtonous Belt' (Bagheri and Damani Gol, 2020) that are contiguous with the Lut block (Bröcker et al., 2014; Bagheri and Damani Gol, 2020). The structure and evolution of this deformed belt and the nature of Sistan's abrupt termination has so far not been studied in detail and is the subject of our field study.

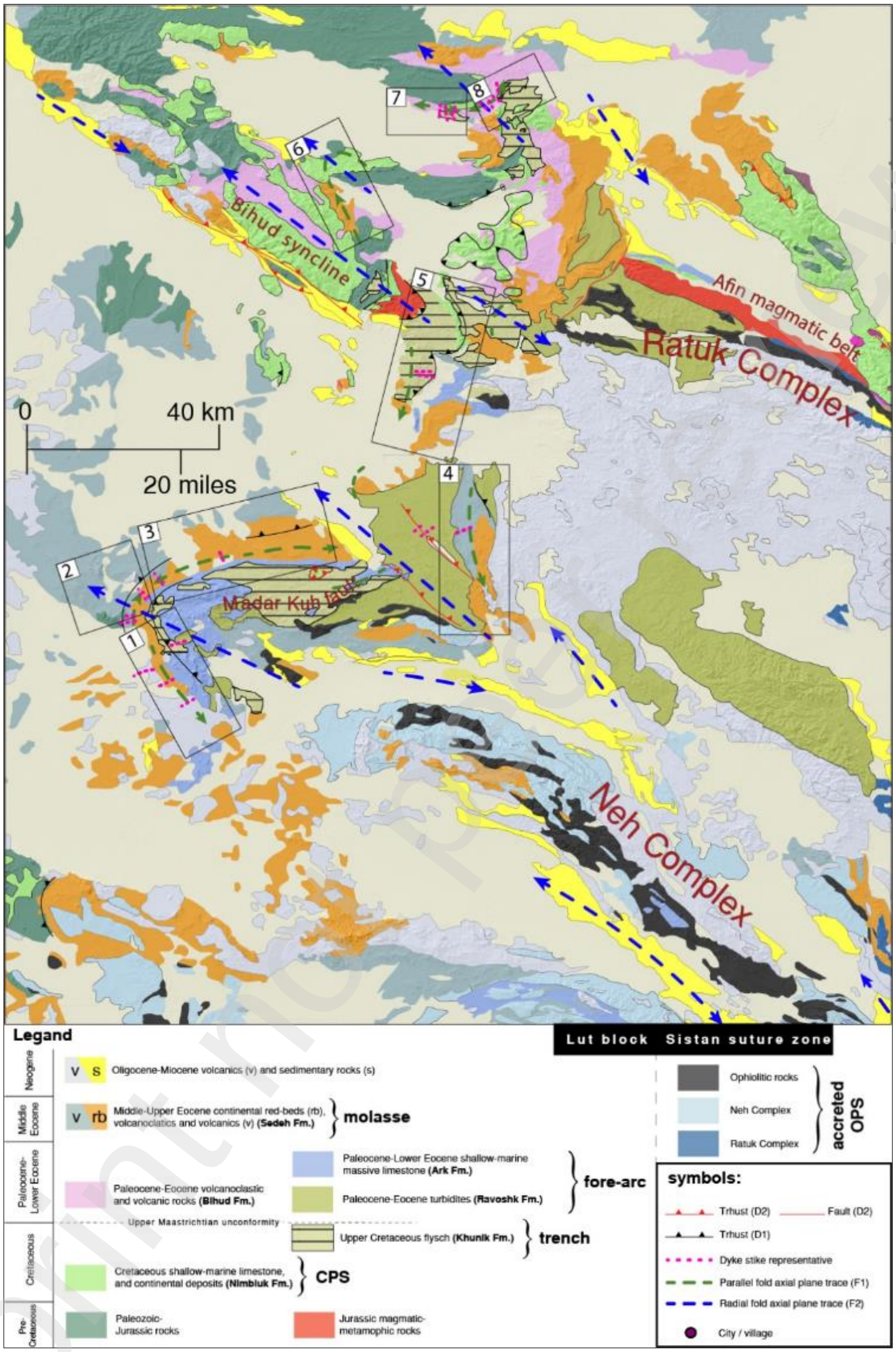

Figure 5. Geological and structural map of northern termination of the Sistan Suture zone and the Neogene basin (bright yellow polygons) located between the northwest-trend structural ridges (Ratuk and Neh complexes), with representative strike of fold axial planes of both radial folds/F2 (blue dashed lines) and parallel folds/F1 (dark green dashed lines) according to the eastern curved belt of the Lut block. Pink dotted lines represent the strike of the dike for each segment. The pink dash-lines are representative of the dikes, cut across the F1 folds. Note the Sedeh Formation is under thrusted by older rock units (Permian-Cretaceous rocks) according to field observations and geological maps. The curved belt is divided into eight segments (1-8), numbered from Khusf area in southwest to Achāni area in northeast of the belt.

3. Results

Our dataset is categorized into three distinct sectors: stratigraphic observations, structural data, and geochronological analysis. Our stratigraphic data predominantly draw from existing literature and have been meticulously reevaluated through extensive field observations. Through this comprehensive examination, we have established a classification system for rock formations that share common lithological attributes and tectonic contexts. This classification serves as a fundamental foundation for our subsequent structural interpretations and analyses.

In our quest to unravel the intricate structural history of the curved belt demarcating the Lut Block and the Sistan Suture, we conducted an extensive field-based structural analysis. This analysis encompassed the detailed study of various geological features, including folds, dikes, and thrust planes. In parallel, we conducted geochronological analyses aimed at enhancing the accuracy and precision of dating the deformation phases within this complex geological setting.

3.1. Stratigraphy

The Lut block contains a stratigraphy comprising continental and shallow open marine sediments from Paleozoic to the Upper Cretaceous. The Cretaceous of the Lut block include shallow-marine carbonates and tidal clastic deposits. These rocks are included in the Nimbluk Formation, which overlie Jurassic formations (Fauvelet & Eftekhar-Nezhad, 1990). Far from the eastern margin of the Lut block, to the east, this Formation is covered by Eocene volcanics and (volcano) clastic sedimentary rocks (Fauvelet & Eftekhar-Nezhad, 1990).

The northern termination of the Sistan Suture Zone is marked by the Khunik Flysch Formation. This Formation comprises green shales, yellowish Orbitholina-bearing sandstones with various sole marks, flaggy, sandy limestones, intraformational conglomerates, and scarce, massive limestone layers, yielded a Turonian-Maastrichtian age (Fauvelet & Eftekhar-Nezhad, 1990). Boulders and olistoliths are locally included within the shales ("wild flysch"). They occupy an extensive northeast-trending belt, from ~65 km west of Birjand city to the west of the Afin belt (Figure 5). To the northeast of the belt, to the north of Qayen, the Khunik Formation is apparently overlying Jurassic rocks of the Lut block. To southwest of this belt, in the Birjand area, rocks of the Khunik Formation cover the Nimblock Formation of the Lut block shelf. The Khunik flysch is interpreted to be deposited in a deep, narrow basin, and was at least in part derived from the adjacent Lut block as it also unconformably covers a folded Jurassic and Lower Cretaceous Lut block margin, in the north (Fauvelet & Eftekhar-Nezhad, 1990).

Unconformably overlying both the Khunik Flysch of the Sistan Suture as well as the Nimbluk Formation of the Lut block is a clastic and carbonate sedimentary sequence of Paleocene to Eocene age that starts with a basal conglomerate. According to the facies these rocks are classified as three different formations that we named Bihud Formation, Ravoshk fore-arc Formation, and the Ark Formation.

The Bihud Formation covers a vast area to the north of the Qayen and comprises basic to intermediate volcanics, interfingering with detrital and volcaniclastic sediments with interlayers of lacustrine limestone, deposited in a non-marine environment. These volcanics and sediments have not been dated but the age of the basal layers of their unconformable cover have been dated as early Eocene (Fauvelet & Eftekhar-Nezhad, 1990).

The Ravoshk Formation crops out along a NE-trending 80-km long belt from west of the Birjand to Boznabad (Figure 5). It comprises a turbidite sequence of sandstone, calcareous shale, intraformational conglomerate and sandy limestone ranging in age from the Upper Maastrichtian to the Paleocene and Lower Eocene. It rests on a basal conglomerate, unconformably overlying

Lower Maastrichtian deposits of the Khunik Formation and ultrabasic rocks and associated metamorphic sediments of Upper Cretaceous age, belonging to the Ratuk and Neh Complex. To the north of Birjand, the Formation is overlain, with a marked unconformity, by a folded series of Eocene molasse-type red beds which are exposed in a NS-trending belt.

The Ark Formation consists of shallow-marine massive nummulitic limestone of the Maastrichtian-Lower Eocene is time-equivalent of the Ravoshk fore arc turbidites, above the Lower Maastrichtian Khunik flysch, also of the Bihud Formation. However, the parallel relationship of these formations has not been observed alongside the folded belt. The lowermost deposits consist of red conglomerates and is overlain by a thick limestone member which passes up to marls and marly limestones. The main and thickest outcrops of the Ark Formation occurred at the southwest of the curved belt, north of the Birjand, close to the Ark village. This limestone is interpreted as deposited in a southeastward deepening open shallow marine environment.

The Ark Formation is overlain by a Middle Eocene-early Oligocene overlapping sequence of mostly molasse-type non-marine rocks of the Sedeh formation, whose thickness exceeds 2000 meters. Two main depositional units are classified under this formation, mutually interfingering, non-marine red-beds, andesitic pyroclastics and flows. These volcanic rocks are regionally associated with dikes that cut the deeper stratigraphic units and are not observed to cut the Oligocene-Pliocene rock units. These unconformably overlie all Maastrichtian-Lower Eocene formations, with a widely recognized basal conglomerate. Deposition in playas, lakes or lagoons are suggested for the red-beds and volcanosedimentary rocks of this formation. This covers the boundary between the Lut and Sistan domains and it was deposited after the closure of the basin (Fauvelet & Eftekhar-Nezhad, 1990).

Finally, extensive Oligocene-Pliocene volcanic and sedimentary rocks unconformably overlie all former formations in a vast area of the north of the Sistan suture. The stratigraphic column of this starts from a basal conglomerate and continues with a sequence primarily made up of red silts and argillites. Its thickness is estimated at 1500 meters (Fauvelet & Eftekhar-Nezhad, 1990).

3.2. Structural analysis

3.2.1. Madar-Kuh Fault

The metamorphosed, folded, and thrusted rocks of the Neh and Ratuk accretionary complexes (Figure 5) abruptly terminate against a curvilinear fault that is perpendicular to the trend of the Sistan suture (Figure 4). We identify this curvilinear fault as the Madar-Kuh fault, which is currently a thrust fault placing the Khunik Flysch Formation and older rock units of the southeastern Lut margin over rocks of the Sistan Accretionary Complex (Figure 6).

The Madar-Kuh Fault is in most places covered by alluvium or Oligocene-Pliocene volcanic and volcano-sedimentary rocks. About 25 km to the north of the city of Birjand, we observed the faults in outcrop. Slices of peridotite of the Neh Complex of 100's of meters thick and a few kilometers long are overthrusted by folded the Khunik Formation turbidite sequences (Figure 6).

The Madar-Kuh Fault is dipping to the northwest suggesting a southeastward thrust direction, although an oblique component cannot be excluded.

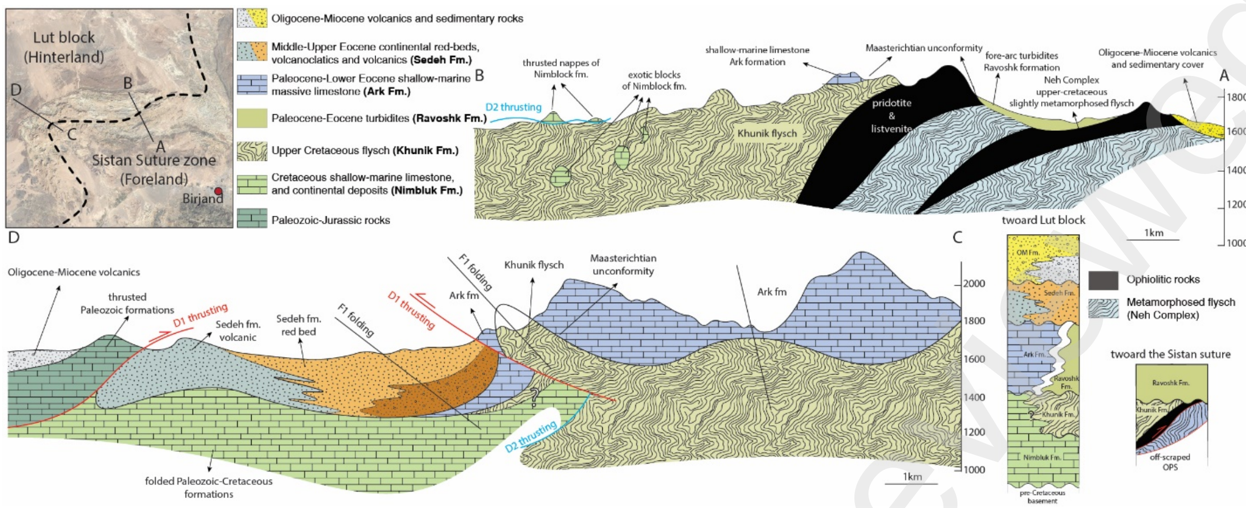

Figure 6. Cross-sections and stratigraphic columns of across the northwestern termination of the Sistan Suture zone, displaying the thrusting of the deformed Lut Block margin onto the Neh Complex of the Sistan Accretionary Complex in the Birjand area; Cross section A-B displays the Madar-Kuh thrust boundary between the Khunik flysch and the Neh complex ophiolite and metamorphosed OPS of Neh Complex. Cross section C-D displays the contractional deformation affecting formations up to Eocene in age at the southeastern margin of the Lut Block. The stratigraphic columns display the stratigraphic relationships and disconformities in the Sistan and Lut domains.

South of the Qayen city (Figure 3), rocks of the Lut margin, the Khunik Flyschoverthrusted onto the Ratuk Complex and overlying ophiolites (Figure 7).

The southeastern margin of the Lut Block adjacent to the Sistan suture zone, has been deformed in a narrow belt of approximately 20 km wide. This region displays two distinct phases of deformation. The older phase consists of thrusts and associated folds that trend parallel to the curvilinear Madar-Kuh fault. South of the city of Qayen, Lower Cretaceous shallow-marine limestones were thrusted southeastward onto the Khunik Flysch, which in turn overthrusted the Ratuk complex (Figure 3 and 10). Towards the southwest, northwest of Birjan, section C-D of Figure 6 shows how the Paleozoic to Jurassic stratigraphic units of the Lut Block, as well as the Paleocene-Eocene Ark Formation are folded and thrusted over the Lower-Middle Eocene Sedeh Formation, both southeastward as well as backthrusted northwestward. These folds and thrusts are parallel to and deform the hanging wall of the Madar-Kuh Fault. Mesoscale recumbent isoclinal folds are located close to thrust contacts (Figure). These overall NE-SW trending first-generation folds and thrusts were previously referred to as 'parallel folds' by Bagheri and Gol (2020). The youngest formation that we observed to be affected by this first generation 'parallel' folding is the Lower to Middle Eocene Sedeh Formation.

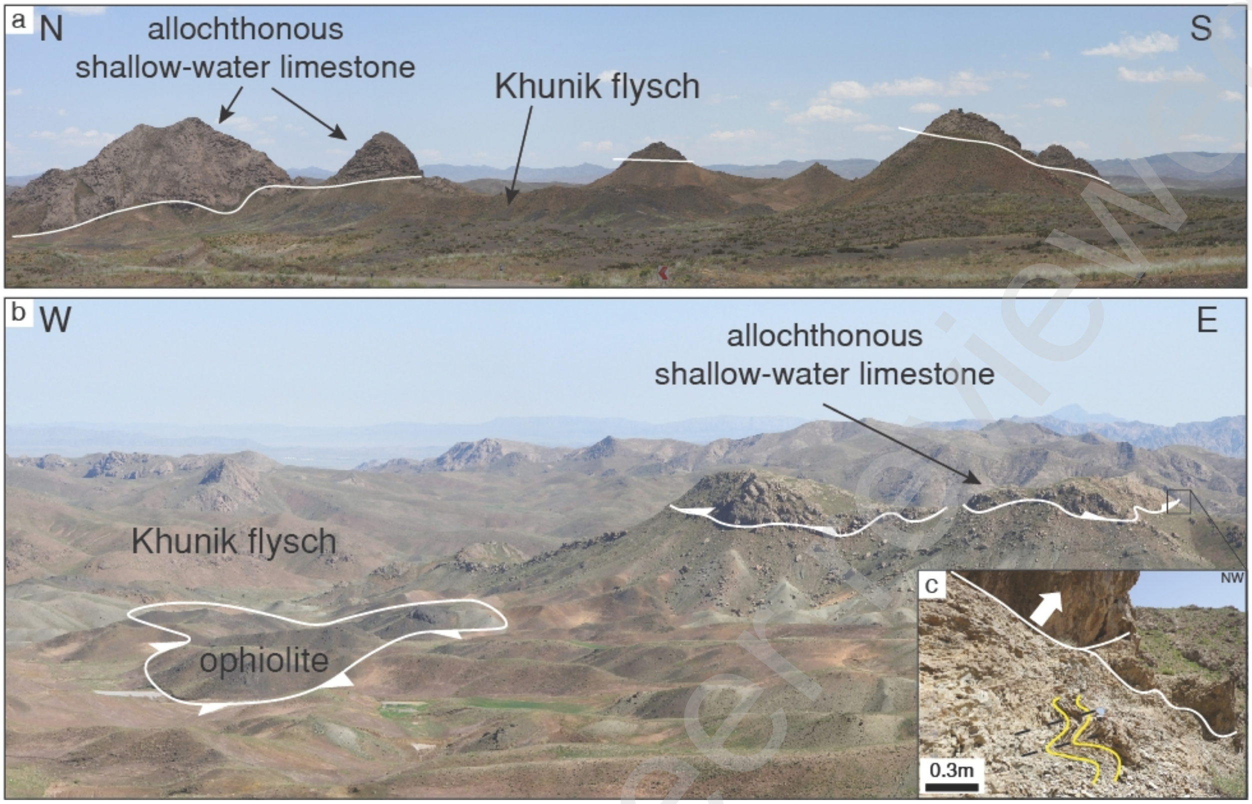

Figure 7. Panoramic views of the Nimbluk Formation allochthonous bodies, originally from the Lut block shelf, located on the Khunik trench-fill flysch. (a & b), (c) a close-up of the intricate isoclinal folds found within the Khunik flysch of the footwall formation.

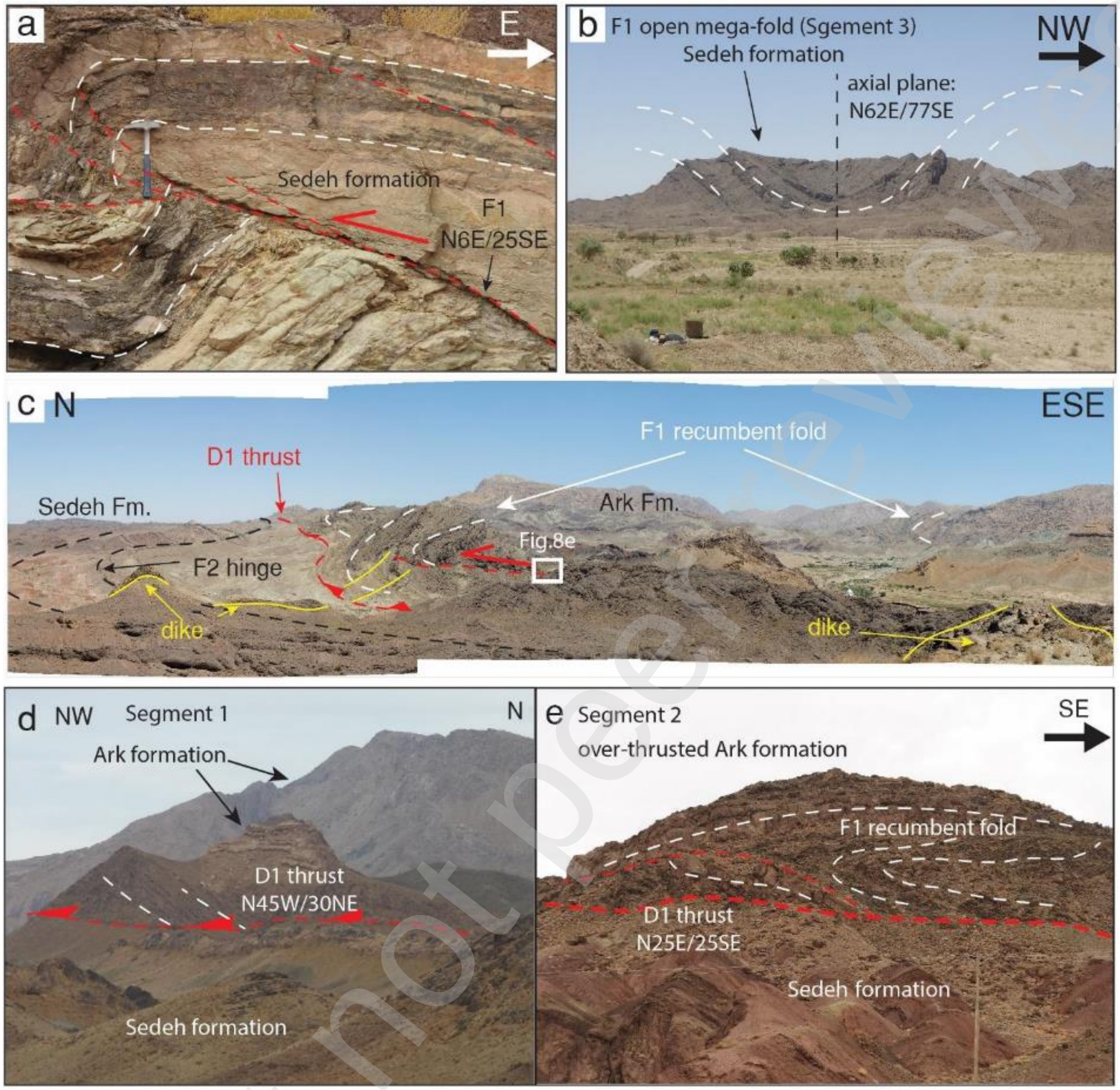

Figure 8. Photographs of key field relationships, (a) a clear thrust surface of the post-Middle Eocene thrusting within the Sedeh Formation in Segment 2, at the hinge of the N-shaped structure, (b) an example of open parallel folds (F1) which deformed the Sedeh Formation on the eastern margin of the Lut block (c), landscape view of post-Middle Eocene thrusting (D1), the hanging-wall recumbent folds, and the radial dikes, from the hinge of F2 folds (segment 2) looking to the segment 3, within the Sedeh formation, (d) thrust faulting (D1) of Ark Formation on the Sedeh formation.

These first generation of folds and thrusts were refolded by smaller-scale folds with fold axes that trend near-perpendicular, NW-SE. This refolding is manifested as plunging antiforms and synforms. This second generation of folds was previously referred to as 'radial folds' by Bagheri and Gol (2020). Our structural observations show that Oligocene to even Pliocene rocks are affected by this second generation folding (Figure), but these post-Eocene rocks display no evidence for the first generation folding. We infer that the curvilinear trace of the Madar-Kuh Fault at the northern termination of the Sistan Suture Zone, is the result of the interference of the two generations of folding (and thrusting) that affected the southeastern Lut Block margin after the early to Middle Eocene.

Along the entire strike of the hanging wall of the Madar-Kuh Fault, the first-generation folds (F1) are cut by swarms of mafic dikes that trend roughly perpendicular to the F1 fold axes. Because the F1 fold axes are refolded and hence curved, the dikes define a fanning pattern (Figure 8.a, c). The dikes vary in width from 1 to 30m and are typically 6-8m wide and exposed lengths may be traced in the field over some 200 m along-strike. The dikes cut through all formations up to the Eocene Sedeh Formation, but we did not observe them in younger formations.

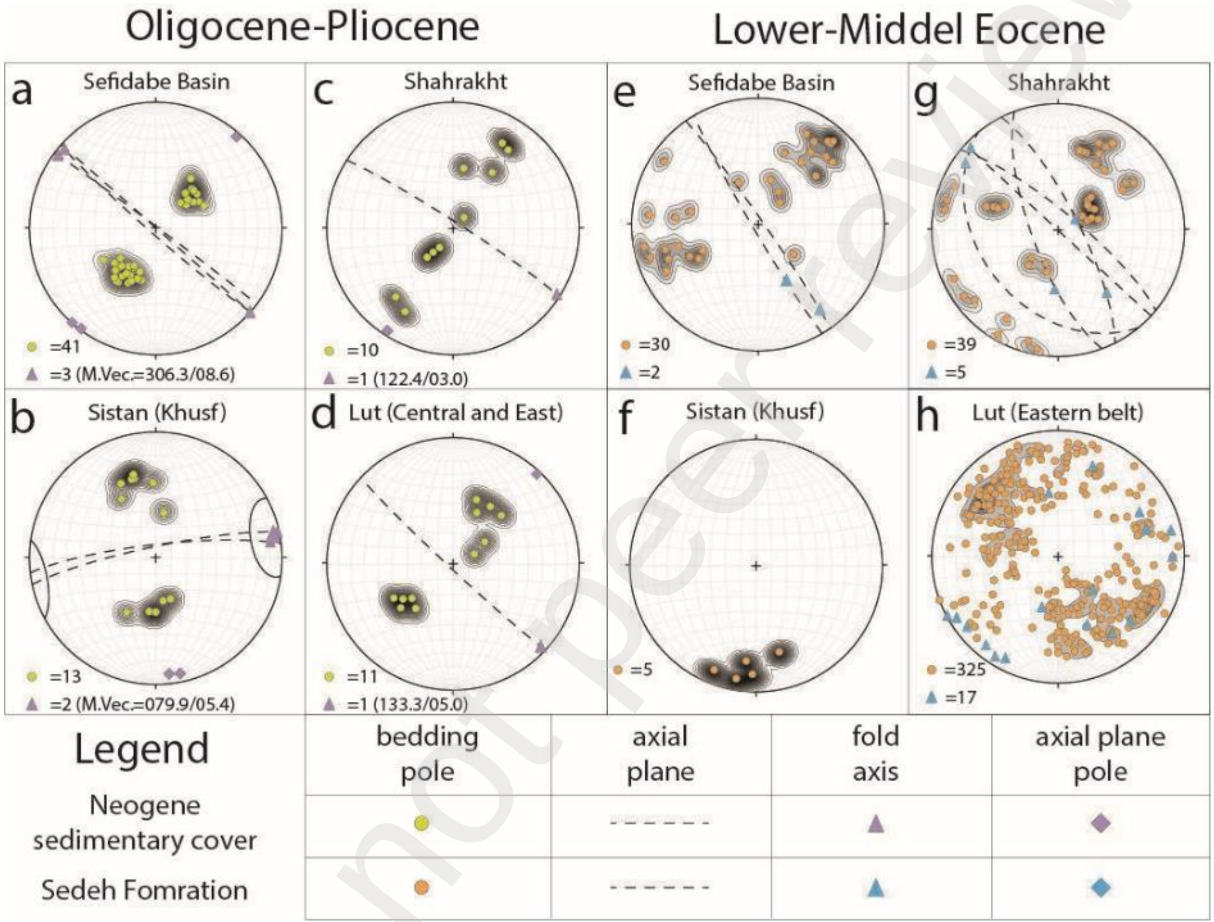

Figure 9. Southern hemisphere equal-area projection of field measurements of Neogene sedimentary cover and the Middle Eocene red beds (Sedeh Formation) of Sistan suture zone and the Lut block. Folding analysis of the Neogene of the Sefidabeh basin (a) comparing to west of the Sistan suture, Khusf region (b), the northeast of the suture, the Esfand region (c), and other region of the Lut block (eastern belt and central Lut) (d); fold analysis of the F1 folds from Sedeh Formation of the Sefidabeh basin with open folds by NW-SE upright axial plane (e); northeast of the suture, the Esfand region by folds with NW-SE axial plane strike, occasionally recumbent and superimposed folds (g); west of the Sistan suture, the Khusf region (f) adjacent to the eastern belt of the Lut block (h). Note the data of the F1 on the curved belt does not represent a unique and simple orientation of the folding axial planes, which is caused by the second generation of folding (F2).

We measured dike orientations as well as the bedding of F1 folds that were cut by these dikes, along the length of the Madar-Kuh hanging wall and performed the orocline test of Pastor-Galan et al. (2017) (Figure 9). This test demonstrates that there is a systematic angular relationship, near-perpendicular, between the F1 fold orientation and dike strike. From this, we infer that the dikes were intruded after F1 folding, but prior to F2 folding. Two dike samples from the north and the south of the study area were collected for U-Pb zircon dating to constrain the minimum age for the first folding and the maximum age for the second folding phase (Figure 10).

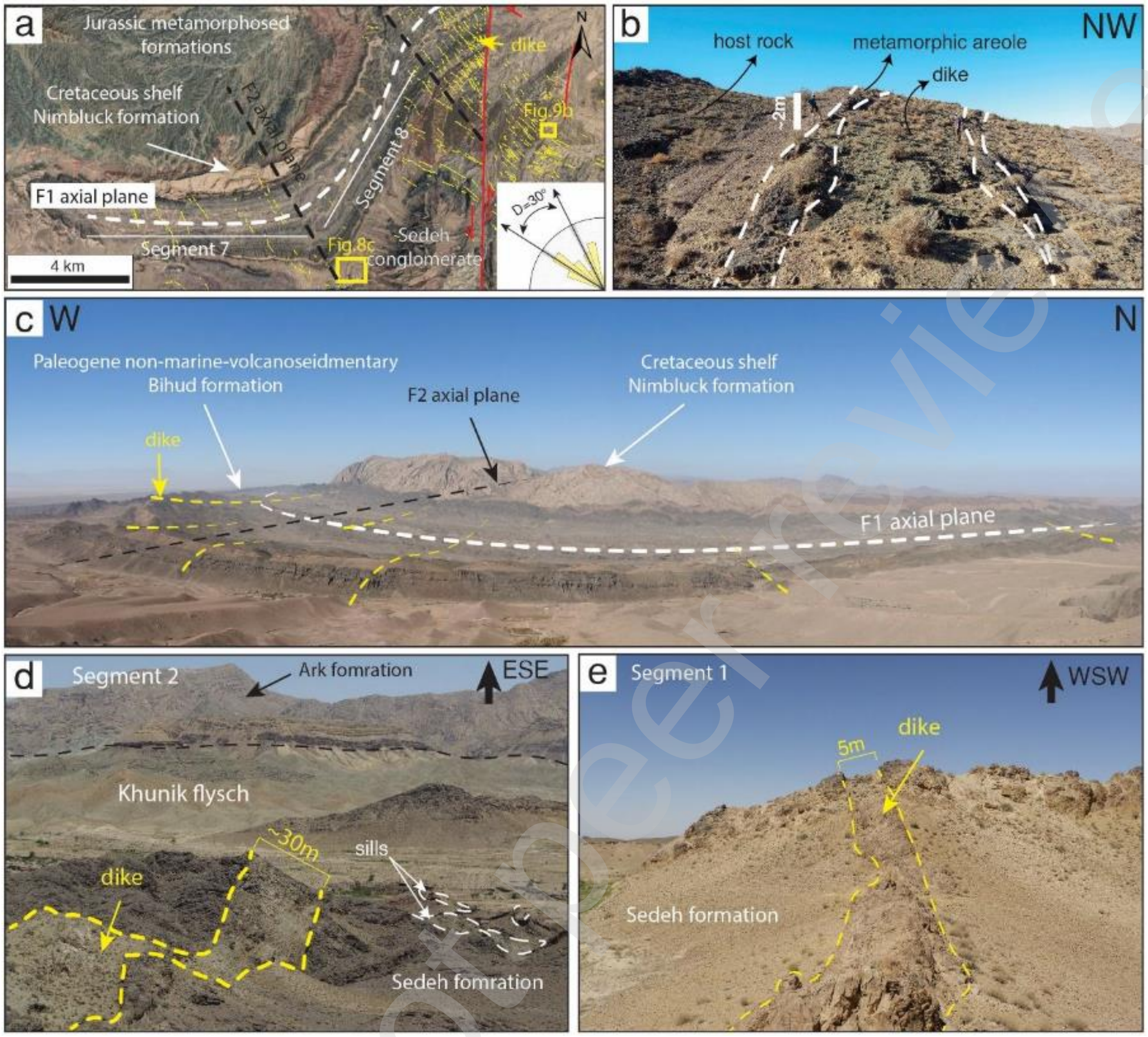

Figure 8. Photographs of key field relationships on the curved belt of the Lut block eastern margin: (a) Google Earth image of dike swarm orthogonally cut the axial plane of the Achāni syncline, (b) a single ~6-meter-thik andesitic dike intruded within the Paleocene-Eocene volcano-sedimentary rocks (Bihud formation) with the metamorphic areole; (c) panorama from the southern convex of the Achāni structure and plotted dikes (yellow dash line) cut through the curved axial plane (F1, white dash line), and the F2 axial plane trace (black dash-line), (d) a E-W striking 30-meter thick andesitic dike intruded within the Sedeh red-beds at the segment 3, and (e) another example of post-Middle Eocene dike joint to a sill cutting the Sedeh Formation at the segment 1.

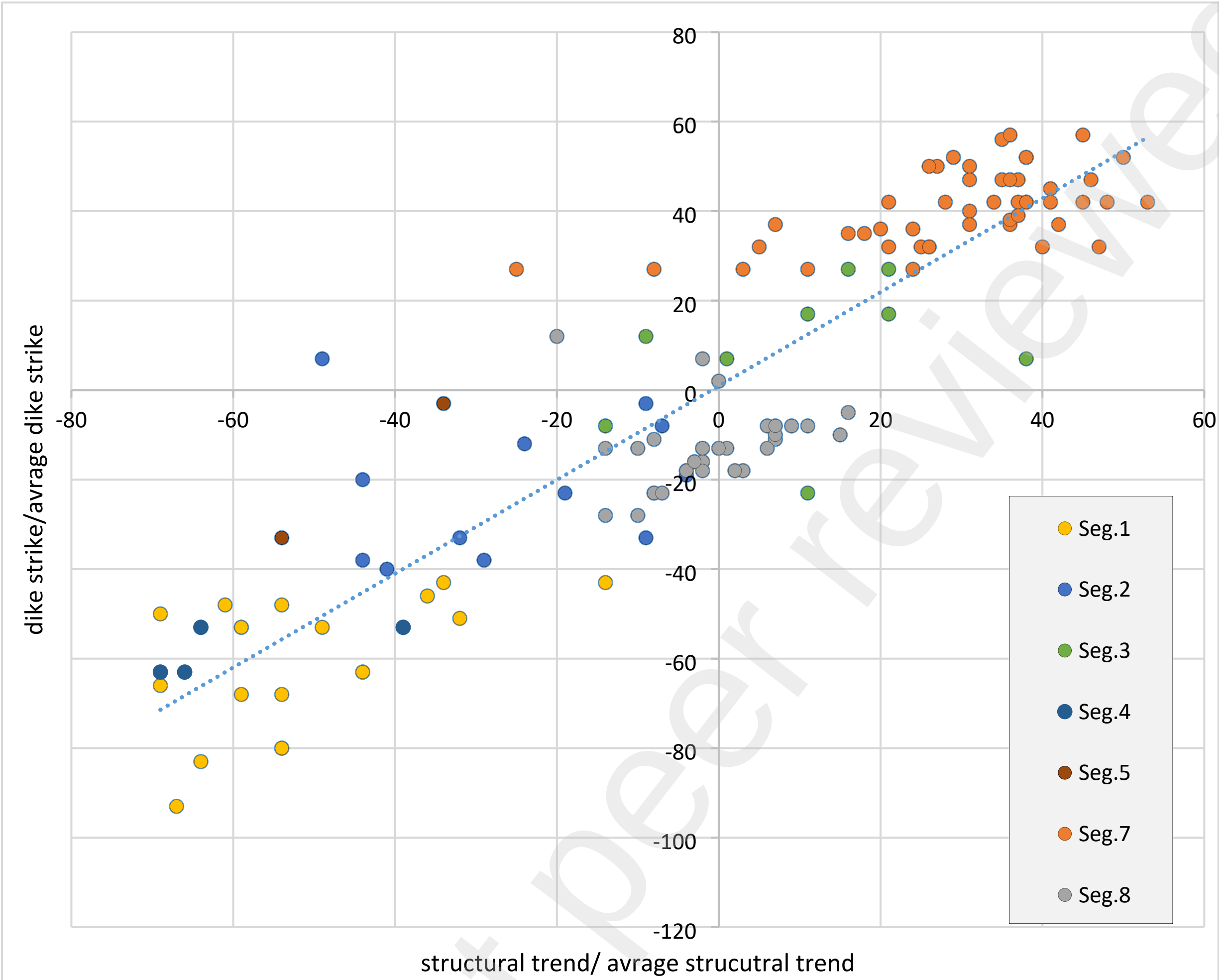

Figure 9. Orocline test (Pastor-Galan et al., 2017) showing a systematic angular relationship between the orientation of F1 fold limbs and cross-cutting dike orientations. This suggests that the dikes were intruded after F1 folding but prior to F2 re-folding.

4. U/Pb dating of dikes

Zircon grains were separated from ~5 kg rock samples by conventional heavy liquid and magnetic techniques, and then picked by hand under a binocular microscope. For all samples, more than 150 zircon grains were randomly selected from over 500 grains, and mounted in epoxy resin, and polished to expose the inner part of the zircon grains. Transmitted and reflected light were used to avoid cracks and inclusions, and cathodoluminescence (CL) images, obtained by a CAMECA electron microscope, were used to identify the morphology and internal texture of the zircon grains.

Zircon U-Pb age analyses were performed by using an Agilent 7500a ICP-MS equipped with a 193-nm laser ablation system at the Institute of Geology and Geophysics, Chinese Academy of Sciences (IGGCAS). The details of analytical procedures were followed method described in Wu et al. (2010). For each sample, at least 30 zircon grains were dated with a spot diameter of 32 um. The standard zircons (91500 and GJ-1) were used to determine the U-Th-Pb ratios and absolute abundances of the analyzed zircon. Data were processed with the GLITTER program (Griffin et al., 2008). The $^{206}Pb/^{238}U$ ages are used for zircons with concordant ages less than

1,100 Ma, and $^{207}Pb/^{206}Pb$ ages are used for zircons when $^{206}Pb/^{238}U$ ages are older than 1,100 Ma. A data plot was conducted by using the Density Plotter program (Vermeesch, 2012). Only the youngest ages from the rim of the zircon crystals were employed as the emplacement age of the dikes. All the U-Pb data are provided in Supplementary Table 1.

Forty-five zircon grains were measured on sample ACH-401 from the northeast end of the parallel fold, 16 zircons yield a concordant $^{206}Pb/^{238}U$ age at 43.1 ± 0.51 Ma (1σ, n = 28, Figure 10). For Sample DR-5b that collected from the southwestern end of the "parallel fold", the ages are scattered, ranging from the late Eocene to the Mesoproterozoic, only 6 zircons (30 analysis) yield a concordant $^{206}Pb/^{238}U$ age of 51.3 ± 1.5 Ma (1σ, n = 6, Figure 10).

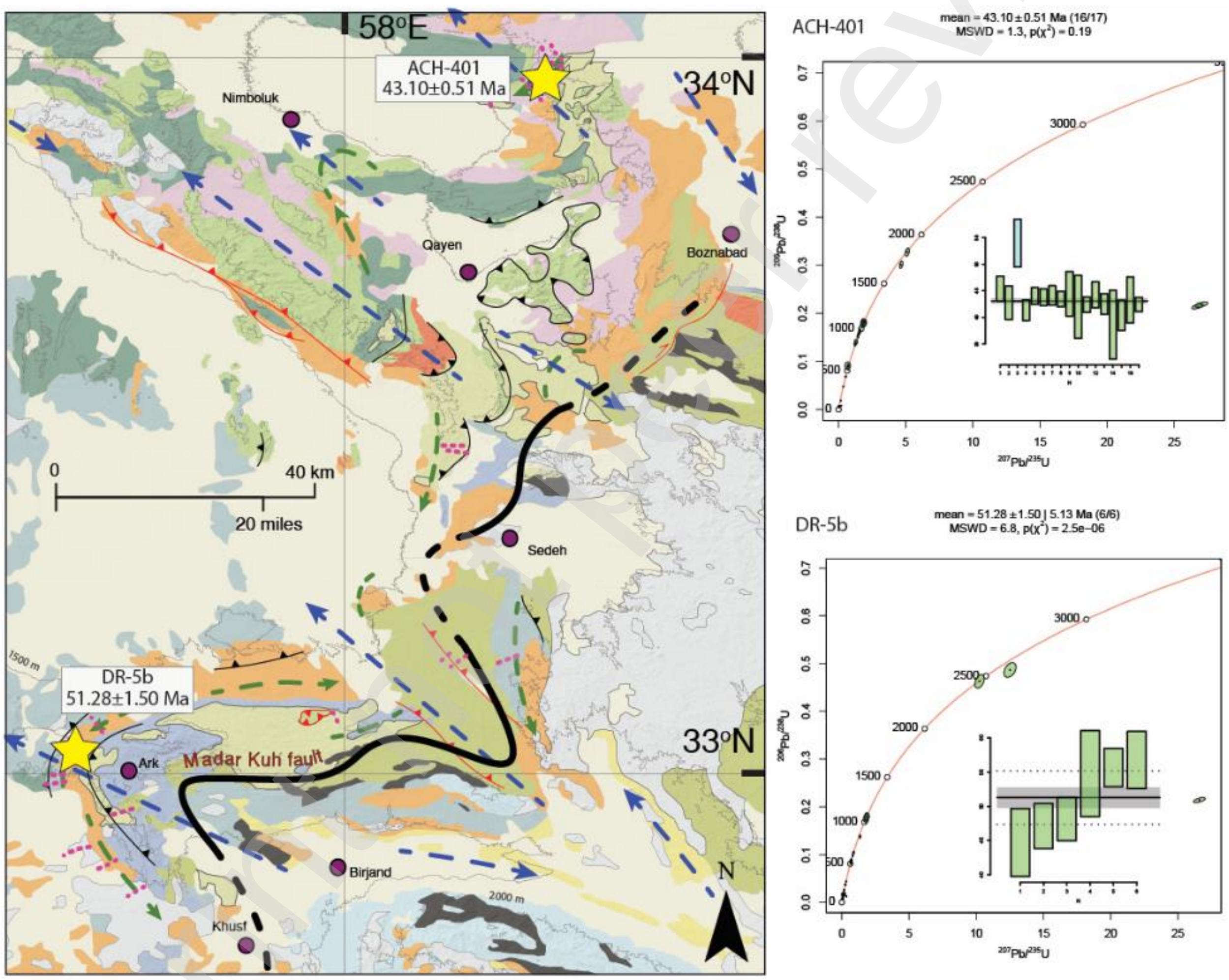

Figure 10. Results of isotopic U-Pb dating of zircon crystals obtained from the dikes cutting F1 folds and being folded by F2 folds.

5. Discussion

In one hand, Bagheri and Gol (2020) explained the northern termination of the suture zone with an oroclinal buckling evolution model. In this scenario, the 200 km wide Sistan suture zone does not terminate in the north and the Sistan OPS curves 180°, surrounded by the Lut block. They argued for this based on the Afin Jurassic magmatic belt and associated metamorphic complexes, interpreting these as a result of Neo-Tethys subduction (Figure 13). Such an orocline requires that the Ratuk complex is also present on the western side of the suture zonem aling the eastern margin of the Lut block (Ozesvart et al., 2020). However, no HP-LT metamorphic rocks have so far discovered at the eastern margin of the Lut block.

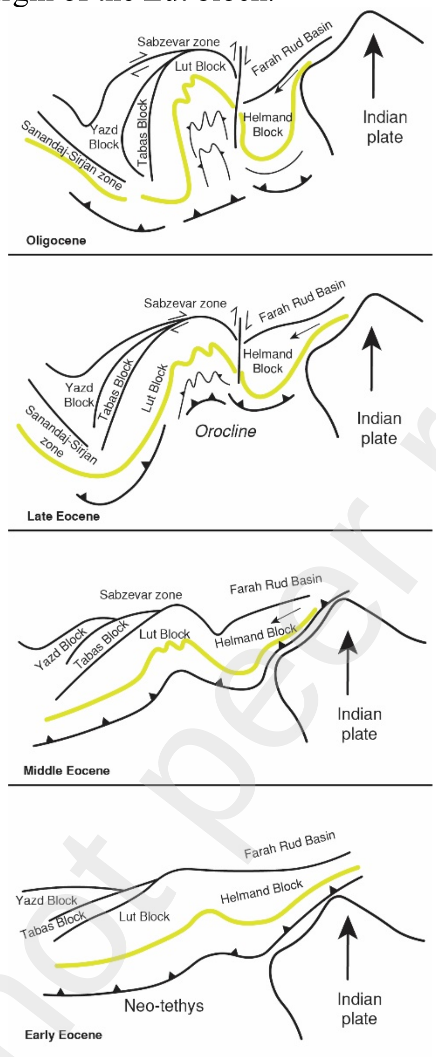

Figure 11. Cartoons illustrating the evolution of the southern active margin of central Eurasia accomodating E-W shortening due to the westward extrusion of the Helmand block away from the Tibetan orogen.

On the other hand, our analysis shows that the Madar-Kuh Fault zone forms an abrupt northern ending of the 750 km long Sistan Suture Zone. Our structural analysis shows that in its modern orientation, the Madar-Kuh Fault Zone is a SE-verging thrust that places shallow-marine rocks and volcanics correlated to the Lut Block, with ages up to the Eocene, over deformed Sistan Suture Zone accretionary prism rocks. In the hanging wall of this fault is a series of parallel folds and thrusts that formed in the same age. This curvilinear Madar-Kuh Fault and associated fold-thrust belt terminates where also the Sistan Suture Zone terminates in the southwest. In other words, this fault appears to be related to the Formation of the suture zone, rather than representing an unrelated younger thrust system. Moreover, our analysis shows that the curvilinear nature of the fault zone reflects a second folding phase that is parallel to the Madar-Kuh Fault Zone and that caused fold interference. Our U-Pb ages of dikes affected by the second, but not by the first folding phase, as well as the ages of the folded strata show that the second phase of folding postdates 43 Ma and that may have occurred in the Neogene. The first folding, and the associated SE ward thrusting of the Lut Block over the NW ward termination of the Sistan Suture Zone occurred in the Early-Mid Eocene, prior to 50 Ma. From this we infer that the thrusting along the Madar-Kuh Fault occurred in the latest stages of, or just after its final closure and the arrest of subduction in the Sistan Suture.

In other words, the Madar-Kuh Fault, during the activity of the Sistan Suture Zone, was a straight fault, striking perpendicular to the strike of the suture zone, without a demonstrable vertical component, but with continental crust on the north(west)ern side, and deep-marine, oceanic rocks on the south(east)ern side. The eastward subduction of the Sistan Ocean below the Helmand Block, from late Cretaceous to Eocene time, must have been associated with major E-W convergence, during which time the Helmand Block advanced towards Iran, and the Sistan Suture Zone rolled back towards the Lut Block. The only tectonic way for a subduction zone to abruptly terminate is against a transform fault, or, more specifically, a subduction transform edge propagator (STEP) Fault (Figure 12), which becomes younger in the direction of the downgoing plate, as treating propagates (Govers & Wortel, 2005). We infer that the Madar-Kuh Fault must represent the youngest portion of the STEP fault that accommodated the westward extrusion of the Helmand Block from western Tibetan architecture (see e.g., Bagheri and Gol, 2020; Şengör et al., 2023) and the westward retreat of the Sistan Subduction Zone relative to the Lut Block (Figure 12). Given the overall N-S strike of the Sistan Suture zone, we suggest that the curvature to NW-SE at its northern termination, as well as the NE-SW strike of the Madar-Kuh Fault result from counterclockwise vertical axis rotation that is well-documented from the Lut Block (Mattei et al. 2012, 2015; Soffel et al. 1996), and that the original orientations were ~N-S and E-W, respectively. We speculate that the eastward continuation of this STEP fault is the Waser (Waras-Panjaw) suture zone between the Helmand Block and the Farah Rud Basin of Afghanistan (Boulin, 1990; Girardeau et al. 1989; Şengör 1984; Stöcklin, 1977, 1989, Tapponier et al. 1981) (Figure 12). The well-documented N-S Neogene shortening in the Kopet Dagh thrust belt of NE Iran (Hollingsworth et al. 2010; Lybéris and Manby, 1999) must have displaced the Madar-Kuh Fault and Sistan Suture zone northward relative to the Afghan orogenic infrastructure, but future detailed restoration of the Iranian-Afghan orogen is required to further evaluate this hypothesis.

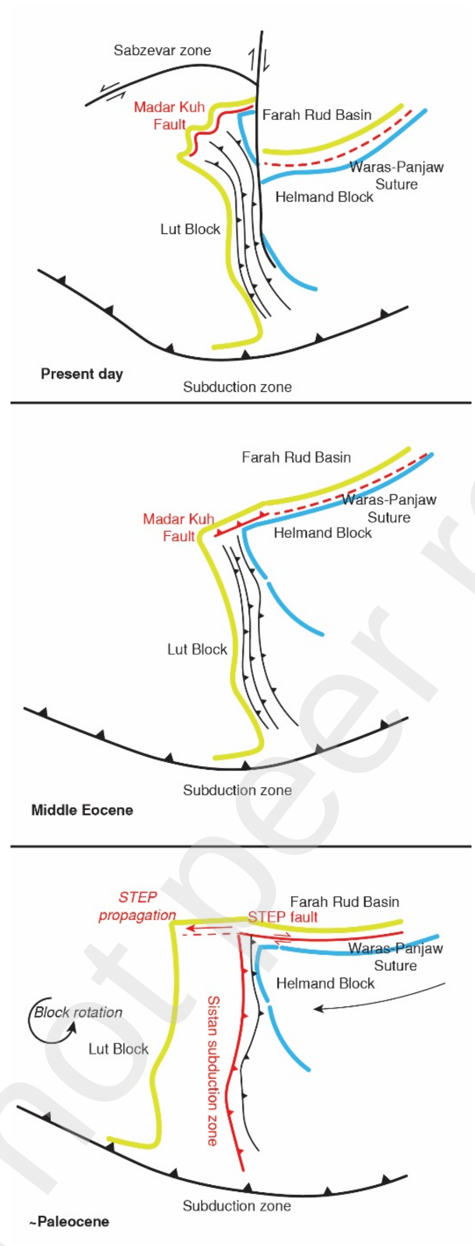

Figure 12. Cartoons illustrating the evolution of the Madar-Kuh Fault at the northern termination of the Sistan Suture Zone as a late-stage STEP fault that propagated from the east during the advance of the Helmand Block that led to the subduction and closure of the Sistan Ocean.

Our data suggest that the Madar-Kuh STEP fault formed along the transition between the Sistan Ocean basin and continental crust of the Lut Block that bounded the ocean to the north. This suggests that the Lut Block had a ~90° kink in its passive margin, which likely represents an older transform fault inherited from its rifting and opening history. Such Formation of a STEP fault along a continent-ocean boundary may comparable to the Miocene STEP fault along the north African margin of Algeria and Morocco that formed during the westward retreat of the Gibraltar slab (Govers and Wortel, 2005; Spakman and Wortel, 2004; van Hinsbergen et al., 2014). The ongoing N-S convergence between Africa and Europe there led to inversion of this STEP fault as a presently active thrust system (Deverchere et al., 2005; Baes et al., 2011). This inversion may form an analogy for the Madar-Kuh thrusting over the Sistan Suture Zone in the latest stages of, or just after subduction, and hence STEP fault propagation, terminated. Its abrupt termination at the Madar-Kuh Fault shows that the Sistan Suture Zone is not contiguous with the isolated remains of the Sabzevar Suture Zone of northern Iran, as sometimes hypothesized (Bröcker et al. 2020; Rossetti et al. 2010). Instead, the Sabzevar suture zone is likely genetically linked to the Nain-Baft, or Inner Zagros suture zone, offset along the large-displacement Great Kavir Fault that also displaced rocks from the Paleo-Tethys suture zone into Central Iran (Bagheri and Stampfli, 2008). The Sistan Suture zone was not the only location of long-lived subduction in Central Iran, and pre-mid Cretaceous paleogeography of the Iranian-Afghan realm must thus have been vastly different from today's. Bagheri and Gol (2020) recently stressed this mobility that must have involved major westward motion of the Helmand block and hypothesized that the abrupt northward end of the Sistan suture zone resulted from isoclinal oroclinal bending (Figure 2) (Bagheri and Gol., 2020). Our observation show that the Sistan accretionary prism is not isoclinally bent around a vertical axis but instead terminates against the Madar-Kuh Fault instead. Regional tectonic block rotations, well-documented in the Lut Block, must have played a significant role in the tectonic evolution of the region (Mattei et al. 2012, 2015), but how and when requires an analysis on a larger scale than in the present study.

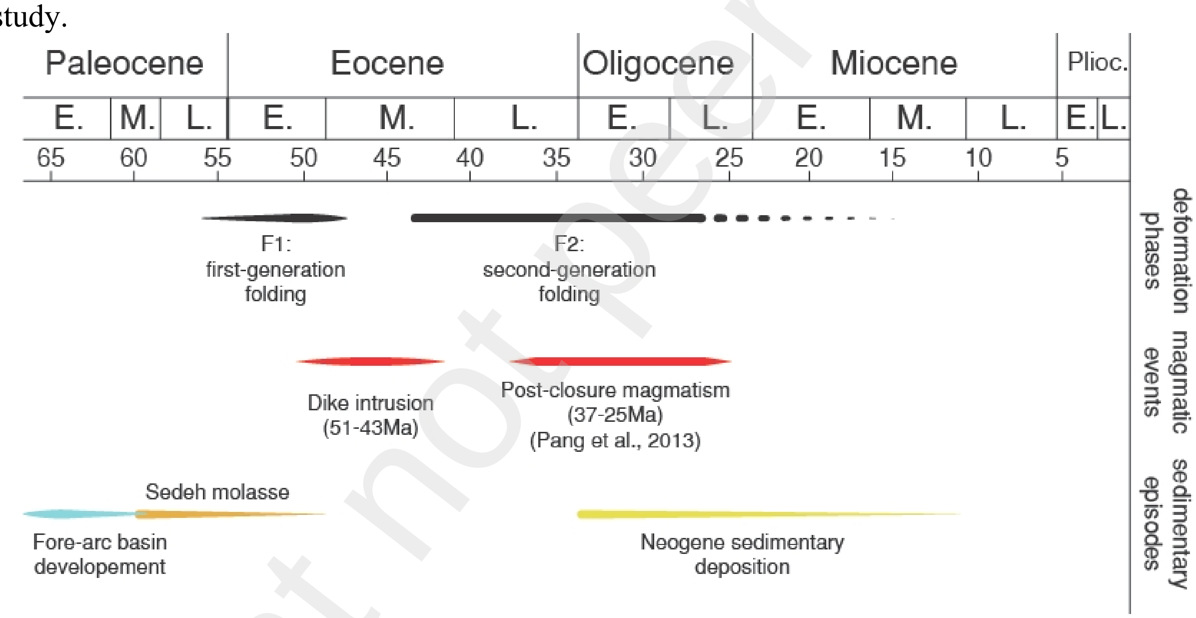

Figure 13. Time line of the deformation phases and magmatic and sedimentary events of the northern termination of Sistan suture zone, since the Paleocene, Post-closer dating results after: (Pang et al., 2013).

Finally, the long-lasting subduction episode that closed the Sistan Ocean, starting at or before ~90 Ma (Bröcker et al., 2013) and lasting until the Eocene, ~50 Ma has important regional implications for the geodynamic evolution of both the tectonic constriction and evolution of the Iranian Plateau as well as the western Tibetan/Pamir Plateau. Although based on the information from the Sistan Suture Zone alone it is not possible to estimate the total amount of subduction involved, the ~E-W convergence that drove its closure requires that the Helmand Block in the hanging wall of the Sistan subduction zone restores far east- or northeastward of its present-day location. This suggests that the Helmand Block was part of the continental tectonic terranes that are identified in the Pamir-Hindu Kush region, and which correlate to the continental fragments that constitute the Tibetan Plateau. Our identification of the northern termination of the Sistan

Suture zone as a STEP fault will aid the reconstruction of the still-enigmatic westward extrusion tectonics from the west-Tibetan orogenic collage, and the associated subduction that closed the Iranian back-arc basins in Cretaceous to Eocene time (
Figure 13).

6. Conclusion

In this paper, we study the tectonic nature of the abrupt northern termination of the enigmatic Sistan Suture Zone in eastern Iran that separates the Iranian Lut Block in the west from the Helmand Block in the east. This suture zone trends nearly perpendicular to the overall E-W trending Neo-Tethyan subduction zone, and hosts a westward, and structurally downward younging, long-lived accretionary prism that is widely interpreted to result from eastward subduction since at least ~90 Ma, until the Middle Eocene, ~50 Ma.

We provide a field study of the abrupt northern termination of this subduction zone, which reveals that the Sistan accretionary prism continues to a sharp boundary formed by the Madar-Kuh thrust fault that emplaced continental margin rocks that correlate with the Lut Block, up to and including the Eocene Ark Formation, over the accretionary prism, and over a deep-marine Paleocene-Eocene turbidite series of the Ravoshk Formation. The Madar-Kuh fault is curvilinear in nature, strikes nearly perpendicular to the overall strike of the Sistan Accretionary Prism, and is associated with folds and thrusts in its hanging wall that strike parallel to the main thrust. The Madar-Kuh fault disappears southwestwards where also the Sistan Accretionary Prism disappears, but continues northeastward beyond the suture zone, between rocks correlated to the Lut and the Helmand blocks. From this we infer that the Madar-Kuh fault is genetically related to Sistan Ocean closure, and not to an unrelated later deformation phase.

We show that the curvilinear nature of the Madar-Kuh fault results from younger refolding. Dikes that cut the first-phase folds and that experienced the second were dated at 51.28±1.5 Ma and 43.10±0.51 Ma, showing that the first folding occurred in the latest stages of Sistan ocean closure, and the second folding phase occurred long after. During Sistan ocean subduction, the Madar-Kuh Fault thus formed a trench-perpendicular, abrupt termination of the subduction zone, which we interpret as a transform fault that formed as the final termination of a STEP-fault, along which the Helmand Block advanced into the Sistan ocean, converging with the Lut Block. We speculate that this STEP fault continues as the Waser suture zone between the Helmand and Farah-Rud blocks of Afghanistan.

Previous paleomagnetic work has revealed that this history was associated with regional vertical axis block rotations. Moreover, the Sistan ocean closure overlapped with Formation of the Sabzevar and Nain-Baft suture zones farther west in Iran. Future regional kinematic restoration is needed to reveal the exact closure history of these oceans, but these ocean closures, likely in back-arc basins north of the main Neo-Tethyan subduction zone, must involve major and long-lived westward motion of the continental blocks of Afghanistan and central Iran in Cretaceous to Eocene time, away from the western Tibetan/Pamir plateau and into the Iranian back-arc basins. Recognizing that the Sistan Suture Zone abruptly ended at a STEP fault provides a kinematic clue towards reconstructing this extrusion history, which will impact the understanding of the dynamics and paleogeography of the Tibetan and Iranian plateaus alike.

Acknowledgments

This work was supported by the research project of Ferdowsi University of Mashhad, Mashhad, Iran (no. 48315), and National Natural Science Foundation of China (no. 42261144673) to S. Li. NL and DJJvH acknowledge NWO Vici grant 865.17.001 to DJJvH. We extend our heartfelt gratitude to Mr. Amir Jalali Nejad, Mr. Amir Sahbaie, Mr. Shams Damani Gol, and Dr. Ali Ahmadi for their invaluable support during field trips and sample collection.

Open Research

Original data of bedding, thrusts and dike plane of the Sedeh Formation generated from this study are openly available in Rojhani, Emad (2024), "Rojhani et al. 2024", Mendeley Data, V1, doi: 10.17632/hzcpdwrnhs.1, Licence: CC BY 4.0.

References

Abdi, M., & Karimpour, M. H. (2013). Petrological Characteristics and timing of Middle Eocene granitic magmatism in Kooh-Shah, Lut block, Eastern Iran. *Acta Geologica Sinica-English Edition*, *87*(4), 1032–1044. https://doi.org/10.1111/1755-6724.12108

Agard, P., Omrani, J., Jolivet, L., Whitechurch, H., Vrielynck, B., Spakman, W., Monié, P., Meyer, B., & Wortel, R. (2011). Zagros orogeny: A subduction-dominated process. *Geological Magazine*, *148*(5–6), 692–725. https://doi.org/10.1017/S001675681100046X

Agard, P., Yamato, P., Jolivet, L., & Burov, E. (2009). Exhumation of oceanic blueschists and eclogites in subduction zones: Timing and mechanisms. *Earth-Science Reviews*, *92*(1–2), 53–79. https://doi.org/10.1016/j.earscirev.2008.11.002

Akrami, M. A., Chaichi, Z., & Haddadan, M. (2005). Geological map of Abiz, scale 1:100,000. *Geological Survey of Iran.*

Alavi-Naini, M. (1980). Shahrakht geological quadrangle map. *Geological Survey of Iran.*

Alavi-Naini, M., & Behruzi, A. (1983). Gonabad geological quadrangle map. In *Geological Survey of Iran:* No. K6.

Allen, M. B. (2021). Arabia-Eurasia Collision. *Encyclopedia of Geology (2nd ed.). Elsevier Inc*. https://doi.org/10.1016/b978-0-12-409548-9.12522-9

Angiboust, S., Agard, P., De Hoog, J. C. M., Omrani, J., & Plunder, A. (2013). Insights on deep, accretionary subduction processes from the Sistan ophiolitic "mélange" (Eastern Iran). *Lithos*, 156–159, 139–158. https://doi.org/10.1016/j.lithos.2012.11.007

Arjmandzadeh, R., Karimpour, M. H., Mazaheri, S. A., Santos, J. F., Medina, J. M., & Homam, S. M. (2011). Two-sided asymmetric subduction; implications for tectonomagmatic and metallogenic evolution of the Lut Block, eastern Iran. *Journal of Economic Geology*, *3*(1), 1–14.

Arvin, M. and Robinson, P.T., 1994. The petrogenesis and tectonic setting of lavas from the Baft ophiolitic mélange, southwest of Kerman, Iran. *Canadian Journal of Earth Sciences,* 31(5), pp.824-834.

Babazadeh, S. A., & De Wever, P. (2004a). Age crétacé des radiolarites de Soulabest dans la suite ophiolitique d'Iran oriental. *Bulletin de La Societe Geologique de France*, *175*(2), 121–129. https://doi.org/10.2113/175.2.121

Babazadeh, S. A., & De Wever, P. (2004b). Radiolarian Cretaceous age of Soulabest radiolarites in ophiolite suite of eastern Iran. *Bulletin de La Societe Geologique de France*, *175*(2), 121–129. https://doi.org/10.1109/MUE.2007.129

Bagheri, S. (2007). The exotic Palaeo-Tethys Terrane in Central Iran: new geological data from Anarak, Jandaq and Posht-e-Badam areas. In *Faculté des Géosciences et de l'environnement* (p. 223). éditeur non identifié.

Bagheri, Sasan, & Damani Gol, S. (2020). The eastern iranian orocline. *Earth-Science Reviews*, *210*(January), 123. https://doi.org/10.1016/j.earscirev.2020.103322

Bagheri, Sasan, & Stampfli, G. M. (2008). The Anarak, Jandaq and Posht-e-Badam metamorphic complexes in central Iran: New geological data, relationships and tectonic implications. *Tectonophysics*, *451*(1–4), 123–155. https://doi.org/10.1016/j.tecto.2007.11.047

Berberian, F., & Berberian, M. (1981). Tectono-plutonic episodes in Iran. In H. K. Gupta & F. M. Delani (Eds.), *Zagros; Hindu Kush; Himalaya: Geodynamic Evolution; Geodynamics Series* (Vol. 3, pp. 5–32). American Geophysical Union. https://doi.org/10.1029/GD003p0005

Berberian, F., Muir, I. D., Pankhurst, R. J., & Berberian, M. (1982). Late Cretaceous and early Miocene Andean-type plutonic activity in northern Makran and Central Iran. *Journal of the Geological Society*, *139*, 605–614. https://doi.org/10.1144/gsjgs.139.5.0605

Berberian, M. (1973). Structural history of Lut Zone*. Geological Survey of Iran. In Tehran, Internal report.*

Berberian, M., & King, G. C. P. (1981). Towards a paleogeography and tectonic evolution of Iran. *Canadian Journal of Earth Sciences*, *18*(2), 210–265. https://doi.org/10.1139/e81-019

Beydokhti, R. M., Karimpour, M. H., Mazaheri, S. A., Santos, J. F., & Klötzli, U. (2015). U-Pb zircon geochronology, Sr-Nd geochemistry, petrogenesis and tectonic setting of Mahoor granitoid rocks (Lut Block, Eastern Iran). *Journal of Asian Earth Sciences*, *111*, 192–205. https://doi.org/10.1016/j.jseaes.2015.07.028

Biabangard, H., Begheri, S., & Karimzaie, J. A. (2020). Petrology and geochemistry of gabbro part of Samsour Ophiolite, South East of Iran. *Iranian Journal of Crystallography and Mineralogy*, *28*(1), 95–110. https://doi.org/10.29252/ijcm.28.1.95

Bina, M. M., Bucur, I., Prevot, M., Meyerfeld, Y., Daly, L., Cantagrel, J. M., & Mergoil, J. (1986). Palaeomagnetism, petrology and geochronology of tertiary magmatic and sedimentary units from Iran. *Tectonophysics*, *121*(2–4), 303–329. https://doi.org/10.1016/0040-1951(86)90050-8

Bonnet, G., Agard, P., Angiboust, S., Monié, P., Jentzer, M., Omrani, J., Whitechurch, H., & Fournier, M. (2018). *Tectonic slicing and mixing processes along the subduction interface: the Sistan example (Eastern Iran)*. . https://doi.org/10.1016/j.lithos.2018.04.016

Boulin, J. (1990). Neocimmerian events in Central and Western Afghanistan. *Tectonophysics*, *175*(4), 285–315. https://doi.org/10.1016/0040-1951(90)90177-A

Bröcker, M., Fotoohi Rad, G., Abbaslu, F., & Rodionov, N. (2014). Geochronology of high-grade metamorphic rocks from the Anjul area, Lut block, eastern Iran. *Journal of Asian Earth Sciences*, *82*, 151–162. https://doi.org/10.1016/j.jseaes.2013.12.021

Bröcker, M., Fotoohi Rad, G., Burgess, R., Theunissen, S., Paderin, I., Rodionov, N., & Salimi, Z. (2013). New age constraints for the geodynamic evolution of the Sistan Suture Zone, eastern Iran. *Lithos*, *170–171*, 17–34. https://doi.org/10.1016/j.lithos.2013.02.012

Buchs, D. M., Bagheri, S., Martin, L., Hermann, J., & Arculus, R. (2013). Paleozoic to Triassic ocean opening and closure preserved in Central Iran: Constraints from the geochemistry of meta-igneous rocks of the Anarak area. *Lithos*, *172–173*, 267–287. https://doi.org/10.1016/J.LITHOS.2013.02.009

Camp, V. E., & Griffis, R. J. (1982). Character, genesis and tectonic setting of igneous rocks in the Sistan suture zone, eastern Iran. *Lithos*, *15*(3), 221–239. https://doi.org/10.1016/0024-4937(82)90014-7

Conrad, G., Montigny, R., Thuizat, R., & Westphal, M. (1981). Tertiary and quaternary geodynamics of southern Lut (Iran) as deduced from palaeomagnetic, isotopic and structural data. *Tectonophysics*, *75*(3–4). https://doi.org/10.1016/0040-1951(81)90272-9

Davoudzadeh, M., & Schmidt, K. (1981). Contribution to the paleogeography and stratigraphy of the Upper Triassic to Middle Jurassic of Iran. *Neues Jahrbuch Für Geologie Und Paläontologie. Abhandlungen*, *162*(2), 137–163.

Davoudzadeh, M., Soffel, H., & Schmidt, K. (1981). On the rotation of the Central-East-Iran microplate. *Neues Jahrbuch Für Geologie Und Paläontologie - Monatshefte*, *1981*(3), 180–192. https://doi.org/10.1127/njgpm/1981/1981/180

Delaloye, M., & Desmons, J. (1980). Ophiolites and mélange terranes in Iran: A geochronological study and its paleotectonic implications. *Test Tectonophysics*, *68*(1–2), 83–111. https://doi.org/10.1016/0040-1951(80)90009-8

Delavari, M. (2013). Different geodynamic settings for Sistan suture zone ophiolitic units: discussion of textural evidences and mineral chemistry of crustal sequence ultramafic-mafic associations. *Petrology*, *4*(16), 39–58.

Delavari, M., Amini, S., Schmitt, A. K., McKeegan, K. D., & Mark Harrison, T. (2014). U-Pb geochronology and geochemistry of Bibi-Maryam pluton, eastern Iran: Implication for the late stage of the tectonic evolution of the Sistan Ocean. *Lithos*, *200–201*(1), 197–211. https://doi.org/10.1016/j.lithos.2014.04.015

Desmons, J., & Beccaluva, L. (1983). Mid-ocean ridge and island-arc affinities in ophiolites from Iran: Palaeographic implications. Complementary reference. *Chemical Geology*, *39*(1–2), 39–63. https://doi.org/10.1016/0009-2541(83)90071-2

Eftekhar-Nezhad, J., & Ruttner, A. (1977). Ferdows geological quadrangle map No. J6. *Geological Survey of Iran.*

Eftekhar-Nezhad, J., & Stocklin, J. (1992). Birjand geological quadrangle map. In *Geological Survey of Iran: No. K8*.

Esmaeily, D. (2001). Petrology and geochronology of Shah-Kuh granite with special references to tin mineralization. *Unpublished Ph. D Thesis, TarbiatModares University*.

Esmaeily, D., Nédélec, A., Valizadeh, M. V., Moore, F., & Cotten, J. (2005). Petrology of the Jurassic Shah-Kuh granite (eastern Iran), with reference to tin mineralization. *Journal of Asian Earth Sciences*, *25*(6), 961–980. https://doi.org/10.1016/j.jseaes.2004.09.003

Etemadi, A., Karimpour, M. H., Malekzadeh Shafaroudi, A., Santos, J. F., Mathur, R., & Ribeiro, S. (2019). U-pb zircon geochronology, geochemistry, and petrogenesis of the hamech intrusions in the kuh-e-shah volcano-plutonic complex, Eastern Iran. *Turkish Journal of Earth Sciences*, *28*(1), 38–59. https://doi.org/10.3906/yer-1710-5

Etemadi, A., Nadermezerji, S., Karimpour, M. H., Malekzadeh Shafaroudi, A., Santos, J. F., & Ribeiro, S. (2020). Geochemistry, petrogenesis, zircon U[sbnd]Pb geochronology and Sr[sbnd]Nd isotopic composition of Kuh-e-Shah volcanic rocks: Implications for an active continental margin along with eastern Iran during the Paleogene. *Lithos*, *378–379*. https://doi.org/10.1016/j.lithos.2020.105778

Fauvelet, E., & Eftekhar-Nezhad, J. (1990). Explanatory text of the Qayen quadrangle map 1:250,000. In *Geological Survey of Iran*.

Fauvelet, E., & Nezhad, J. E. (1992). *Explanatory text of the Gonabad Quadrangle Map, 1: 250,000*. Geological Survey of Iran.

Fotoohi Rad, G. R., Droop, G. T. R., Amini, S., & Moazzen, M. (2005). Eclogites and blueschists of the Sistan Suture Zone, eastern Iran: A comparison of P-T histories from a subduction mélange. *Lithos*, *84*(1–2), 1–24. https://doi.org/10.1016/j.lithos.2005.01.007

Fotoohi Rad, G. R., Droop, G. T. R., & Burgess, R. (2009). Early Cretaceous exhumation of high-pressure metamorphic rocks of the Sistan Suture Zone, eastern Iran. *Geological Journal*, *44*(1), 104–116. https://doi.org/10.1002/gj.1135

Freund, R. (1970). Rotation of Strike Slip Faults in Sistan, Southeast Iran. *The Journal of Geology*, *78*(2), 188–200. https://doi.org/10.1086/627500

Gass, I. G. (1977). The evolution of the Pan African crystalline basement in NE Africa and Arabia. *Journal of the Geological Society*, *134*(2), 129–138. https://doi.org/10.1144/gsjgs.134.2.0129

Ghodsi, M. R., Boomeri, M., Bagheri, S., Ishiyama, D., & Corfu, F. (2016). Geochemistry, zircon U-Pb age, and tectonic constraints on the Bazman granitoid complex, southeast Iran. *Turkish Journal of Earth Sciences*, *25*(4), 311–340. https://doi.org/10.3906/yer-1509-3

Gholami, N., Bagheri, S., & Heyhat, M. R. (2015). The Intruduction of the Ark nappe-thrust: a different glance at the tectonics of the northwest of the Birjand. *18th Symposium of Geological Society of Iran*. https://civilica.com/doc/391424

Girardeau, J., Marcoux, J., & Montenat, C. (1989). The Neo-Cimmerian Ophiolite Belt in Afghanistan and Tibet: Comparison and Evolution. *Tectonic Evolution of the Tethyan Region*, 477–504.

https://doi.org/10.1007/978-94-009-2253-2_19

Guillou, Y., Maurizot, P., Vaslet, D., & Villéon, H. (1983). Gazik geological quadrangle map. In *Geological Survey of Iran: Vol. 1/250000* (Issue 250).

Hollingsworth, J., Fattahi, M., Walker, R., Talebian, M., Bahroudi, A., Bolourchi, M.J., Jackson, J. and Copley, A., 2010. Oroclinal bending, distributed thrust and strike-slip faulting, and the accommodation of Arabia–Eurasia convergence in NE Iran since the Oligocene. *Geophysical Journal International*, 181(3), pp.1214-1246.

Hushmand-Zadeh, A. (1969). Métamorphisme et granitisation du massif Chapedony (Iran Central) *(Doctoral dissertation, Faculte des Sciences de l'Université de Grenoble).*

Jackson, J., & McKenzie, D. (1984). Active tectonics of the Alpine—Himalayan Belt between western Turkey and Pakistan. *Geophysical Journal International*, *77*(1), 185–264. https://doi.org/10.1111/j.1365-246X.1984.tb01931.x

Javidi Moghaddam, M., Karimpour, M. H., Malekzadeh Shafaroudi, A., Santos, J. F., & Corfu, F. (2021). Middle Eocene magmatism in the Khur region (Lut Block, Eastern Iran): implications for petrogenesis and tectonic setting. *International Geology Review*, *63*(9), 1051–1066. https://doi.org/10.1080/00206814.2019.1708815

Javidi Moghaddam, M., Karimpour, M. H., Malekzadeh Shafaroudi, A., Santos, J. F., & Mendes, M. H. (2019). Geochemistry, Sr-Nd isotopes and zircon U-Pb geochronology of intrusive rocks: Constraint on the genesis of the Cheshmeh Khuri Cu mineralization and its link with granitoids in the Lut Block, Eastern Iran. *Journal of Geochemical Exploration*, *202*, 59–76. https://doi.org/10.1016/j.gexplo.2019.04.001

Jentzer, M., Agard, P., Bonnet, G., Monié, P., Fournier, M., Whitechurch, H., Omrani, J., Zarrinkoub, M. H., Khatib, M. M., Kohansal, R., Couto, D. Do, Godbillot, C., & Ninkabou, D. (2022). The North Sistan orogen (Eastern Iran): Tectono-metamorphic evolution and. *Gondwana Research*, *January*. https://doi.org/10.1016/j.gr.2022.04.004

Jentzer, M., Whitechurch, H., Agard, P., Ulrich, M., Caron, B., Zarrinkoub, M. H., Kohansal, R., Miguet, L., Omrani, J., & Fournier, M. (2020). Late Cretaceous calc-alkaline and adakitic magmatism in the Sistan suture zone (Eastern Iran): Implications for subduction polarity and regional tectonics. *Journal of Asian Earth Sciences*, *204*(February), 104588. https://doi.org/10.1016/j.jseaes.2020.104588

Jones, A. G. (1961). Reconnaissance geology of part of West Pakistan. *A Colombo Plan Cooperative Project. Toronto, Canada: Government of Canada*.

Jung, D., Keller, J., Khorasani, R., Marcks, C., Baumann, A., & Horn, P. (1983). Petrology of the Tertiary Magmatic Activity in the Northern Lut Area, East Iran. *Neues Jahrbuch Für Geologie Und Paläontologie - Abhandlungen*, *168*(2–3), 417–467. https://doi.org/10.1127/njgpa/168/1984/417

Karimpour, M. H., Stern, C., Farmer, L., & Saadat, S. (2011). Review of age, Rb-Sr geochemistry and petrogenesis of Jurassic to Quaternary igneous rocks in Lut Block, Eastern Iran. *Geopersia*, *1*(1), 19–54. https://doi.org/10.22059/JGEOPE.2011.22162

Karimzadeh, H., Rahgoshay, M., & Monsef, I. (2020). Mineralogy, geochemistry and petrogenesis of mantle peridotites of nehbandan ophiolitic complex, east of Iran. *Journal of Economic Geology*, *12*(2), 157–176. https://doi.org/10.22067/ECONG.V12I2.76889

Keshtgar, shahriar, Bagheri, S., & Boomeri, M. (2016). Tectonic history of the Mahi Rud (Cheshme-ostad) complex according to new structural data, East of Iran. *Journal of Tectonics*, *1*(4), 63–76. https://doi.org/10.22077/jt.2016.797

Keshtgar, S., Bagheri, S., & Boomeri, M. (2019). Tectonic setting of Mahi Rud Volcano-plutonic Complex: Different insight into the geodynamic history of East Iran. *Scientific Quarterly Journal, GEOSCIENCES*, *113*(3), 131–144. https://doi.org/10.22071/gsj.2018.94653.1217

Khademi, seyyedeh N., Bagheri, S., Gorgij, M. N., Ozsvart, P., & Jafari., S. (2020). Tectonics of the eastern edge of the Lut Zone in Nehbandan area; example of an ancient convergent plate margin architecture. *Journal of Tectonics*, *3*(12), 1–21. https://doi.org/10.22077/jt.2020.1556

Kluyver, M. H., Tirrul, R., Chance, P. N., Johns, G. W., & Mexiner, H. M. (1983). *Explanatory text of the Naybandan quadrangle map 1250,000* (No. J8). Geological Survey of Iran.

Kokaly, R. F., King, T. V. V.., & Hoefen, T. M. (2013). Surface Mineral Maps of Afghanistan Derived from HyMap Imaging Spectrometer Data , Version 2 *(Issue 186, p. 36). US Department of the Interior, US Geological Survey.*

Krumsiek, K. (1976). Zur Bewegung der Iranisch-Afghanischen Platte. *Geologische Rundschau*, *65*(1), 909–929. https://doi.org/10.1007/bf01808504

Kurzawa, T., Bröcker, M., Fotoohi Rad, G., Berndt, J., & Lisker, F. (2017). Cretaceous high-pressure metamorphism and low-pressure overprint in the Sistan Suture Zone, eastern Iran: Additional temperature estimates for eclogites, geological significance of U-Pb zircon ages and Rb-Sr constraints on the timing of exhumation. *Journal of Asian Earth Sciences*, *147*, 332–344. https://doi.org/10.1016/j.jseaes.2017.07.051

latifi, Z., Foroughi, F., Motamedalshariati, M., & Raeisossadat, S. N. (2018). Calcareous nannofossils biostratigraphy of Lower Cretaceous deposits of east of Iran, NW of Qayen (Nimbolook stratigraphic section). *Journal of Geoscience*, *27*(107), 41–50. https://doi.org/10.22071/gsj.2018.63752

Li, S., Advokaat, E. L., van Hinsbergen, D. J. J., Koymans, M., Deng, C., & Zhu, R. (2017). Paleomagnetic constraints on the Mesozoic-Cenozoic paleolatitudinal and rotational history of Indochina and South China: Review and updated kinematic reconstruction. *Earth-Science Reviews*, *171*, 58–77. https://doi.org/10.1016/j.earscirev.2017.05.007

Lotfi, M. (1982). *Geological and geochemical investigations on the volcanogenic Cu, Pb-Zn, Sb ore-mineralizations in the Shurab-Galechah and Northwest of Khur (Lut, East Iran)*.

Lyberis, N. and Manby, G., 1999. Oblique to orthogonal convergence across the Turan block in the post-Miocene. *AAPG bulletin,* 83(7), pp.1135-1160.

Mahmoudi, S., Masoudi, F., Corfu, F., & Mehrabi, B. (2010). Magmatic and metamorphic history of the Deh-Salm metamorphic Complex, Eastern Lut block, (Eastern Iran), from U-Pb geochronology. *International Journal of Earth Sciences*, *99*(6), 1153–1165. https://doi.org/10.1007/s00531-009-0465-x

Mattei, M., Cifelli, F., Muttoni, G. and Rashid, H., 2015. Post-Cimmerian (Jurassic–Cenozoic) paleogeography and vertical axis tectonic rotations of Central Iran and the Alborz Mountains. *Journal of Asian Earth Sciences*, 102, pp.92-101.

Mattei, M., Cifelli, F., Muttoni, G., Zanchi, A., Berra, F., Mossavvari, F. and Eshraghi, S.A., 2012. Neogene block rotation in central Iran: Evidence from paleomagnetic data. *GSA Bulletin*, 124(5-6), pp.943-956.

Maurizot, P. (1980). Explanatory text of the Gazik quadrangle map 1:250,000. *Geological Survey of Iran.*

Maurizot, P., Fauvelet, E., & Eftekhar-Nezhad, J. (1990). Explanatory text of the Shahrakht quadrangle map 1:250,000. *Geological Survey of Iran.*

Mazhari, S. A., & Safari, M. (2013). High-K calc-alkaline plutonism in Zouzan, NE of Lut block, Eastern Iran: An evidence for arc related magmatism in Cenozoic. *Journal of the Geological Society of India*, *81*(5), 698–708. https://doi.org/10.1007/s12594-013-0091-x

McQuarrie, N., & Van Hinsbergen, D. J. J. (2013). Retrodeforming the Arabia-Eurasia collision zone: Age of collision versus magnitude of continental subduction. *Geology*, *41*(3), 315–318.

https://doi.org/10.1130/G33591.1

Moghadam, H. S., & Stern, R. J. (2015). Ophiolites of Iran: Keys to understanding the tectonic evolution of SW Asia: (II) Mesozoic ophiolites. *Journal of Asian Earth Sciences*, *100*, 31–59. https://doi.org/10.1016/j.jseaes.2014.12.016

Mohammadi, A., Burg, J. P., Bouilhol, P., & Ruh, J. (2016). U-Pb geochronology and geochemistry of Zahedan and Shah Kuh plutons, southeast Iran: Implication for closure of the South Sistan suture zone. *Lithos*, *248–251*, 293–308. https://doi.org/10.1016/j.lithos.2016.02.003

Montenat, C. (2009). The Mesozoic of Afghanistan. *GeoArabia*, *14*(1), 147–210.

Moradi Noghondar, M., Karimpour, M., Farmer, G., & Stern, C. (2011). SrNd isotopic characteristic, U-Pb zircon geochronology, and petrogenesis of Najmabad Granodiorite batholith, Eastern Iran. *Journal of Economic Geology*, *3*(2), 127–145.

Moslempour, M. E., Khalatbari-jafari, M., & Dabiri, R. (2012). Constraints on the Petrogenesis of Nosrat-Abad Ophiolite. *Iranian Journal of Earth Sciences*. http://www.iaujournals.ir/article_522842_0c2ccdc9dc9df39e46a64e99c6871848.pdf

Nabiei, E., & Bagheri, S. (2013). Tectonic Evolution of East Margin of Lut Block in Nosratabad. *Bulletin of Environment, Pharmancology and Life Scences*, *2*(October), 78–86.

Nadermezerji, S., Karimpour, M. H., Malekzadeh Shafaroudi, A., Francisco Santos, J., Mathur, R., & Ribeiro, S. (2018). U–Pb geochronology, Sr–Nd isotopic compositions, geochemistry and petrogenesis of Shah Soltan Ali granitoids, Birjand, Eastern Iran. *Chemie Der Erde*, *78*(3), 299–313. https://doi.org/10.1016/j.chemer.2018.08.003

Najafi, A., Karimpour, M. H., Ghaderi, M., Stern, C., & Farmer, L. (2014). U-Pb zircon geochronology, Rb-Sr and Sm-Nd isotope geochemistry, and petrogenesis of granitoid rocks at Kajeh prospecting area, northwest Ferdows: Evidence for Upper Cretaceous magmatism in Lut block. *Journal of Economic Geology*, *1*(6), 107–135. https://doi.org/10.22067/econg.v6i1.24415

Nicholson, K. N., Khan, M., & Mahmood, K. (2010). Geochemistry of the Chagai-Raskoh arc, Pakistan: Complex arc dynamics spanning the Cretaceous to the Quaternary. *Lithos*, *118*(3–4), 338–348. https://doi.org/10.1016/j.lithos.2010.05.008

Nikbakht, S., Biabanghard, H., & Bagheri, S. (2021). Petrology and geochemistry of Siahjangal ophiolite, northeastern Taftan volcano. *Iranian Journal of Geology*.

Omidianfar, S., Monsef, I., Rahgoshay, M., Zheng, J., & Cousens, B. (2020). The Middle Eocene high-K magmatism in Eastern Iran Magmatic Belt: constraints from U-Pb zircon geochronology and Sr-Nd isotopic ratios. *International Geology Review*, *62*(13–14), 1751–1768. https://doi.org/10.1080/00206814.2020.1716272

Ozsvárt, P., Bahramnejad, E., Bagheri, S., & Sharifi, M. (2020). New Albian (Cretaceous) radiolarian age constraints for the Dumak ophiolitic mélange from the Shuru area, Eastern Iran. *Cretaceous Research*, *111*. https://doi.org/10.1016/j.cretres.2020.104451

Pang, K. N., Chung, S. L., Zarrinkoub, M. H., Khatib, M. M., Mohammadi, S. S., Chiu, H. Y., Chu, C. H., Lee, H. Y., & Lo, C. H. (2013). Eocene-Oligocene post-collisional magmatism in the Lut-Sistan region, eastern Iran: Magma genesis and tectonic implications. *Lithos*, *180–181*, 234–251. https://doi.org/10.1016/j.lithos.2013.05.009

Pang, K. N., Chung, S. L., Zarrinkoub, M. H., Mohammadi, S. S., Yang, H. M., Chu, C. H., Lee, H. Y., & Lo, C. H. (2012). Age, geochemical characteristics and petrogenesis of Late Cenozoic intraplate alkali basalts in the Lut-Sistan region, eastern Iran. *Chemical Geology*, *306–307*, 40–53. https://doi.org/10.1016/j.chemgeo.2012.02.020

Pang, K. N., Chung, S., Zarrinkoub, M. H., Khatib, M. M., Mohammadi, S. S., Lee, H., Chu, C., & Lin, I. (2011). Eocene-Oligocene calcalkaline magmatism in the Lut-Sistan region, eastern Iran: petrogenesis and tectonic implications. *AGU Fall Meeting Abstracts*.

Pirouz, M., Avouac, J. P., Hassanzadeh, J., Kirschvink, J. L., & Bahroudi, A. (2017). Early Neogene foreland of the Zagros, implications for the initial closure of the Neo-Tethys and kinematics of crustal shortening. *Earth and Planetary Science Letters*, *477*, 168–182. https://doi.org/10.1016/j.epsl.2017.07.046

Pudsey, C. J. (1986). The Northern Suture, Pakistan: Margin of a Cretaceous island arc. *Geological Magazine*, *123*(4), 405–423. https://doi.org/10.1017/S0016756800033501

Raisossadat, S. N., Mosavinia, A., khazaei, A., & Asadi, S. (2020). Biostratigraphy of Cretaceous deposits based on ammonites in Southwest of Qayen area (Qumenjan section). *Journal of Stratigraphy and Sedimentology Researches*. https://doi.org/10.22108/jssr.2020.122202.1155

Ramezani Abbakhsh, T., Malekzadeh Shafaroudi, A., & Karimpour, M. H. (2018). Geology, mineralization, geochemistry, and petrology of monzodioritc dikes in Hatamabad copper occurrence, northeast of Qaen. *Iranian Journal of Crystallography and Mineralogy*, *26*(2), 409–422. https://doi.org/10.29252/ijcm.26.2.409

Ratschbacher, L., Frisch, W., Neubauer, F., Schmid, S. M., & Neugebauer, J. (1989). Extension in compressional orogenic belts: The eastern Alps. *Geology*, *17*(5), 404–407. https://doi.org/10.1130/0091-7613(1989)017

Ratschbacher, Lothar, Merle, O., Davy, P., & Cobbold, P. (1991). Lateral extrusion in the eastern Alps, Part 1: Boundary conditions and experiments scaled for gravity. *Tectonics*, *10*(2), 245–256. https://doi.org/10.1029/90TC02622

Reyre, D., & Mohafez, S. (1972). *A first contribution of the NIOC-ERAP agreements to the knowledge of Iranian geology*. Editions Technip Paris.

Richter, B., & Fuller, M. (1996). Palaeomagnetism of the Sibumasu and Indochina blocks: Implications for the extrusion tectonic model. *Geological Society Special Publication*, *106*(1), 203–224. https://doi.org/10.1144/GSL.SP.1996.106.01.13

Rojhani, E., Bagheri, S., Hinsbergen, D., Azizi, H., Ghaemi, F., Lom, N., & Qayyum, A. (2021). Age of the Eastern Iranian oroclinal Buckling inferred from a U235/Pb207 dating on radial dikes in the Qayen Area. *EGU General Assembly 2021*. https://doi.org/10.5194/egusphere-egu21-14258

Rosenberg, F. (1981). Geochemische and petrologische underssuchungen und magmatiten der intrusion Bejestan ostiran diplomarabeit. *Mineralogy and Petrology*, 122–149.

Rossetti, F., Nasrabady, M., Vignaroli, G., Theye, T., Gerdes, A., Razavi, M. H., & Vaziri, H. M. (2010). Early Cretaceous migmatitic mafic granulites from the Sabzevar range (NE Iran): Implications for the closure of the Mesozoic peri-Tethyan oceans in central Iran. *Terra Nova*, *22*(1), 26–34. https://doi.org/10.1111/j.1365-3121.2009.00912.x

Rowshanravan, J., Shojai kaveh, N., & Bahremand, M. (2006). 1: 100000 Geological map of Mousaviyeh. In *Geological Survey of Iran*.

Saccani, E., Delavari, M., Beccaluva, L., & Amini, S. (2010). Petrological and geochemical constraints on the origin of the Nehbandan ophiolitic complex (eastern Iran): Implication for the evolution of the Sistan Ocean. *Lithos*, *117*(1–4), 209–228. https://doi.org/10.1016/j.lithos.2010.02.016

Sahandi, M. R. (1992). Explanatory text of the Deh-Salm (Chah Vak) geological quadrangle map 1: 250,000, # K9. In *Geological Survey of Iran*.

Sargazi, M., Bagheri, S., & Ma, X. (2022). Oligocene calc-alkaline lamprophyres and K-rich association in the eastern Iranian ranges: Products of low-degree melting of subduction-modified lithospheric mantle in post-orogenic setting. *Lithos*, *430–431*, 106864. https://doi.org/10.1016/j.lithos.2022.106864

Schreiber, A., Weippert, D., Wittekindt, H. P., & Wolfart, R. (1972). Geology and Petroleum Potentials of Central and South Afghanistan. *American Association of Petroleum Geologists Bulletin*, *56*(8), 1494–1519. https://doi.org/10.1306/819a40f6-16c5-11d7-8645000102c1865d

Şengör, A. M.C. (1990). A new model for the late Palaeozoic-Mesozoic tectonic evolution of Iran and implications for Oman. *Geological Society Special Publication*, *49*(1), 797–831. https://doi.org/10.1144/GSL.SP.1992.049.01.49

Şengör, A. M. C. (1979). Mid-Mesozoic closure of Permo-Triassic Tethys and its implications. *Nature*, *279*(5714), 590–593. https://doi.org/10.1038/279590a0

Şengör, A. M. C. (1984). The cimmeride orogenic system and the tectonics of Eurasia. *Special Paper of the Geological Society of America*, *195*, 1–74. https://doi.org/10.1130/SPE195-p1

Şengör, A.M.C., Altıner, D., Zabcı, C., Sunal, G., Lom, N., Aylan, E., Öner, T. (2023). On the nature of the Cimmerian Continent. *Earth-Science Reviews 104520*. https://doi.org/10.1016/j.earscirev.2023.104520

Shirdashtzadeh, N., Furnes, H., Miller, N.R., Dantas, E.L., Torabi, G. and Meisel, T.C., 2022. Subduction initiation of the Neo-Tethys Ocean in Central Iran based on U-Pb geochronology, geochemical and Nd isotope data of the Ashin ophiolite. *Ofioliti*, 47(2).

Siddiqui, R. H., Jan, M. Q., Khan, M. A., Kakar, M. I., & Foden, J. D. (2017). Petrogenesis of the Late Cretaceous Tholeiitic Volcanism and Oceanic Island Arc Affinity of the Chagai Arc, Western Pakistan. *Acta Geologica Sinica*, *91*(4), 1248–1263. https://doi.org/10.1111/1755-6724.13358

Siehl, A. (2017). Structural setting and evolution of the Afghan orogenic segment - A review. In *Geological Society Special Publication* (Vol. 427, Issue 1, pp. 57–88). Geological Society of London. https://doi.org/10.1144/SP427.8

Soffel, H. C., Davoudzadeh, M., & Rolf, C. (1992). A new polar wander path of the Central East Iran Microplate (CEIM) and its tectonic interpretation. *Geosci Sci QJ Geol Surv Iran*, *2*(5), 2–24.

Soffel, H. C., Davoudzadeh, M., Rolf, C., & Schmidt, S. (1996). New palaeomagnetic data from Central Iran and a Triassic palaeoreconstruction. *Geologische Rundschau*, *85*, 293–302.

Soffel, H.C. and Förster, H.G., 1980. Apparent polar wander path of Central Iran and its geotectonic interpretation. *Journal of geomagnetism and geoelectricity*, 32(Supplement3), pp. SIII117-SIII135.

Soffel, H. C., & Förster, H. G. (1984). Polar Wander Path of the Central-East-Iran Microplate Including New Results. *Neues Jahrbuch Für Geologie Und Paläontologie - Abhandlungen*, *168*(2–3), 165–172. https://doi.org/10.1127/njgpa/168/1984/165

Stampfli, G. M., Marcoux, J., & Baud, A. (1991). Tethyan margins in space and time. *Palaeogeography, Palaeoclimatology, Palaeoecology*, *87*(1–4), 373–409. https://doi.org/10.1016/0031-0182(91)90142-E

Stampfli, Gérard M. (2000). Tethyan oceans. *Geological Society Special Publication*, *173*, 1–23. https://doi.org/10.1144/GSL.SP.2000.173.01.01

Stöcklin, J. (1968). Structural History and Tectonics of Iran. *American Association of Petroleum Geologists Bulletin*, *52*(7), 1229–1258. https://doi.org/doi:10.2514/6.1977-211

Stöcklin, J. (1974). Possible Ancient Continental Margins in Iran. *The Geology of Continental Margins*, 873–887. https://doi.org/10.1007/978-3-662-01141-6_64.

Stöcklin, J., (1977). Structural correlation of the Alpine ranges between Iran and Central Asia. In: Livra à la Mémoire de Albert F. de Lapparent. Mémoire hors-série 8, Société Géologique de France, 333-353.

Stöcklin, J, Eftekhar-Nezhad, J., & Hushmand-Zadeh, A. (1972). *Geological Reconnaissance Map of Central Lut, Geological Survey of Iran, Tehran*. Geological Survey of Iran.

Stöcklin, Johan, & Mabavi, M. H. (1973). *Tectonic map of Iran*. Geological Survey of Iran.

Stöcklin, Jovan. (1981). A brief report on geodynamics in Iran. *Zagros Hindu Kush Himalaya Geodynamic Evolution*, *3*(6), 70–74. https://doi.org/https://doi.org/10.1029/GD003p0070

Stöcklin, Jovan. (1989). Tethys Evolution in the Afghanistan-Pamir Region. *Tectonic Evolution of the Tethyan Region*, *25*(3), 241–264. https://doi.org/10.1007/978-94-009-2253-2_13.

Tapponnier, P., Mattauer, M., Proust, F. & Cassaigneau, C. (1981). Mesozoic ophiolites, sutures, and large-scale tectonic movements in Afghanistan. *Earth and Planetary Science Letters*, 52, 355-71.

Tapponnier, P., Peltzer, G., Le Dain, A. Y., Armijo, R., & Cobbold, P. (1982). Propagating extrusion tectonics in Asia: new insights from simple experiments with plasticine. *Geology*, *10*(12), 611–616. https://doi.org/10.1130/0091-7613(1982)10<611:PETIAN>2.0.CO;2

Tarkian, M., Lotfi, M., & Baumann, A. (1983). *Tectonic, magmatism and the Formation of mineral deposits in the central Lut, east Iran*.

Tirrul, R., Bell, I. R., Griffis, R. J., & Camp, V. E. (1983). The Sistan suture zone of eastern Iran. *Geological Society of America Bulletin*, *94*(1), 134–150. https://doi.org/10.1130/0016-7606(1983)94<134:TSSZOE>2.0.CO;2

Tirrul, R., Griffis, R. J., & Camp, V. E. (1980). Geology of the Zabol Quadrangle, 1.250, 000. In *Geological Survey of Iran* (Vol. 180).

Toulabi Nejad, E., Ahmadi Khalaji, A., Ebrahimi, M., Biabangard, H., & Esmaeili, R. (2021). Petrology , geochemistry , source and tectonic setting of Malek Chah Ruii granitoid (East of Lut Block). *Petrology*, *45*. https://doi.org/https://doi.org/10.22108/ijp.2020.124366.1196

Walker, R., & Jackson, J. (2004). Active tectonics and late Cenozoic strain distribution in central and eastern Iran. *Tectonics*, *23*(5), 1–24. https://doi.org/10.1029/2003TC001529

Walker, R. T., Gans, P., Allen, M. B., Jackson, J., Khatib, M., Marsh, N., & Zarrinkoub, M. (2009). Late Cenozoic volcanism and rates of active faulting in eastern Iran. *Geophysical Journal International*, *177*(2), 783–805. https://doi.org/10.1111/j.1365-246X.2008.04024.x

Wan, B., Chu, Y., Chen, L., Liang, X., Zhang, Z., Ao, S., & Talebian, M. (2021). Paleo-Tethys subduction induced slab-drag opening the Neo-Tethys: Evidence from an Iranian segment of Gondwana. *Earth-Science Reviews*, *221*(August), 103788. https://doi.org/10.1016/j.earscirev.2021.103788

Zanchi, A., Malaspina, N., Zanchetta, S., Berra, F., Benciolini, L., Bergomi, M., Cavallo, A., Javadi, H. R., & Kouhpeyma, M. (2015). The Cimmerian accretionary wedge of Anarak, Central Iran. *Journal of Asian Earth Sciences*, *102*, 45–72. https://doi.org/10.1016/j.jseaes.2014.08.030

Zanchi, A., Zanchetta, S., Berra, F., Mattei, M., Garzanti, E., Molyneux, S., Nawab, A., & Sabouri, J. (2009). The Eo-Cimmerian (Late? Triassic) orogeny in North Iran. *Geological Society Special Publication*, *312*, 31–55. https://doi.org/10.1144/SP312.3

Zarrinkoub, M. H., Pang, K. N., Chung, S. L., Khatib, M. M., Mohammadi, S. S., Chiu, H. Y., & Lee, H. Y. (2012). Zircon U-Pb age and geochemical constraints on the origin of the Birjand ophiolite, Sistan suture zone, eastern Iran. *Lithos*, *154*, 392–405. https://doi.org/10.1016/j.lithos.2012.08.007